Electronic Effects on the β-Alkyl Migratory Insertion Reaction of *para*-Substituted Styrene Methyl Palladium Complexes

Francis C. Rix, Maurice Brookhart,* and Peter S. White

Contribution from the Department of Chemistry, University of North Carolina at Chapel Hill, Chapel Hill, North Carolina 27599-3290

Received August 11, 1995[⊗]

Abstract: The β-methyl migratory insertion chemistry of a series of *cis*-coordinated styrene methyl complexes of palladium [(phen)Pd(CH_3)(*p*-X-$C_6H_4CH{=}CH_2$)$^+$Ar′$_4$B$^-$ (**2X**) (phen = 1,10-phenanthroline; X = CF_3, Cl, H, CH_3, OCH_3; Ar′ = 3,5-$(CF_3)_2C_6H_3$)] has been investigated. Complexes **2X** are prepared *in situ* from the addition of *p*-X-styrene to CD_2Cl_2 solutions of (phen)Pd(CH_3)(OEt_2)$^+$Ar′$_4$B$^-$ (**1**). The X-ray structure of **1** has been determined [$P2_1/c$; a = 16.460(4) Å, b = 18.911(3) Å, c = 17.374(3) Å; β = 117.996(14)°; V = 4775.2(15) Å^3; Z = 4] at −78 °C. The rearrangement of **2X**, via β-CH_3 migratory insertion then arene coordination, to yield (phen)Pd(η^3-CH(CH_2-CH_3)(C_6H_4-*p*-X)$^+$Ar′$_4$B$^-$ (**3X**) has been studied by ^{1}H NMR spectroscopy. The rearrangement is accelerated by electron-withdrawing groups; a Hammett analysis at −29.2 °C reveals that log k values are best fit by σ^p parameters: ρ^p = 1.1 ± 0.1, r = 0.992. The *anti*-isomer of **3H** has been structurally characterized: $P2_1$/n; a = 13.950(4) Å, b = 15.582(5) Å, c = 24.004(8) Å; β = 101.961(24)°; V = 5105(3) Å^3; Z = 4. Complex **3H** reacts further with styrene to form (phen)Pd(η^3-CH(CH_3)(C_6H_5)$^+$Ar′$_4$B$^-$ (**4**) and (*E*)-β-methylstyrene; kinetic and isotopic labeling experiments have been employed to determine the mechanism of this benzyl exchange reaction. The relative binding affinities of the *p*-X-styrenes of **2X** have been determined for the equilibria *p*-X-$C_6H_4CH{=}CH_2$ + **2H** ⇌ C_6H_5-$CH{=}CH_2$ + **2X** at −66 °C. The electron-rich styrenes bind tightest to Pd; a Hammett plot of these equilibrium constants yields ρ^p = −2.2 ± 0.1 and r = 0.999. The kinetic and thermodynamic data indicate that both the ground and transition-states are stabilized by electron-rich styrenes and, of the two, the substituent effects are greatest in the ground-states. Since the relative rates are determined by the relative differences in energy of the ground and transition states, the migratory insertion reaction of **2X** is accelerated by styrenes bearing electron-withdrawing substituents.

Introduction

β-Alkyl migratory insertion (eq 1) and β-H elimination (eq 2) are two reactions intimately involved in the dimerization, oligomerization and polymerization of olefins.[1−12] Although the β-alkyl migratory insertion is thought to be widespread, there have been only a small number of direct observations of olefin alkyl complexes that undergo this reaction.[11−22] The most common examples of the β-alkyl migratory insertion have been

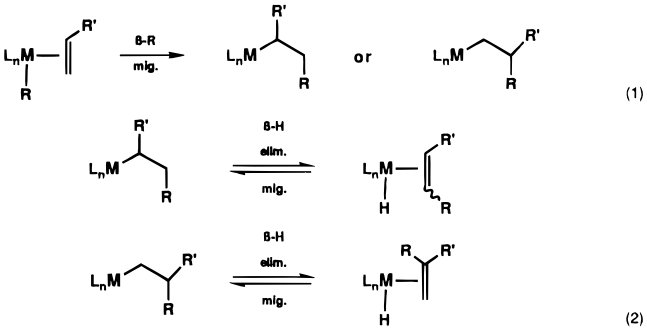

precursors[11,12,16] and intermediates in late transition metal-catalyzed olefin dimerizations[11,14,15,21] and polymerizations.[12,13]

No systematic study has been undertaken of the β-alkyl migratory insertion reaction of a series of olefin alkyl complexes in which the electronic properties of the alkene have been varied. However, the closely related β-H migratory insertion reaction of a series of β-substituted styrene hydride complexes have been examined by Halpern[23] and Bercaw[24,25] for the migratory insertions of $(PPh_3)_2$(Cl)Rh(H)(*p*-X-styrene)[23] and *exo* and *endo*-Cp_2Nb(H)(*p*-X-styrene),[24,25] respectively; systematic electronic effects on the stabilities of ground and transition-states were observed and rationalized.

Similar studies of β-alkyl migratory insertion reactions should provide additional insight into the factors governing these

[⊗] Abstract published in *Advance ACS Abstracts,* February 15, 1996.

(1) Watson, P.; Roe, D. C. *J. Am. Chem. Soc.* **1982**, *104*, 6471.
(2) Watson, P. L. *J. Am. Chem. Soc.* **1982**, *104*, 337.
(3) Jordan, R. F.; Bajgur, C. S.; Willet, R.; Scott, B. J. *J. Am. Chem. Soc.* **1986**, *108*, 7410.
(4) Jeske, G.; Lauke, H.; Mauermann, H.; Swepston, P. N.; Schumann, H.; Marks, T. J. *J. Am. Chem. Soc.* **1985**, *107*, 8091.
(5) Jeske, G.; Harald, L.; Mauermann, H.; Swepston, P. N.; Schumann, H.; Marks, T. J. *J. Am. Chem. Soc.* **1985**, *107*, 8111.
(6) Soto, J.; Steigerwald, M. J.; Grubbs, R. J. *J. Am. Chem. Soc.* **1982**, *104*, 4479.
(7) Clawson, L.; Soto, J.; Buchwald, S. L.; Steigerwald, M. L.; Grubbs, R. H. *J. Am. Chem. Soc.* **1985**, *107*, 3377.
(8) Schmidt, G. F.; Brookhart, M. *J. Am. Chem. Soc.* **1985**, *107*, 1443.
(9) Burger, B. J.; Thompson, M. E.; Cotter, W. D.; Bercaw, J. E. *J. Am. Chem. Soc.* **1990**, *112*, 1566.
(10) Thorn, D. L.; Hoffmann, R. *J. Am. Chem. Soc.* **1978**, *100*, 2079.
(11) Rix, F. C.; Brookhart, M. *J. Am. Chem. Soc.* **1995**, *117*, 1137.
(12) Johnson, L. K.; Killian, C. M.; Brookhart, M. *J. Am. Chem. Soc.* **1995**, *117*, 6414.
(13) Brookhart, M.; Volpe, A. F.; Lincoln, D. M.; Hovarth, I. T.; Millar, J. M. *J. Am. Chem. Soc.* **1990**, *112*, 5634.
(14) Brookhart, M.; Lincoln, D. M. *J. Am. Chem. Soc.* **1988**, *110*, 8719.
(15) Brookhart, M.; Hauptman, E.; Lincoln, D. *J. Am. Chem. Soc.* **1992**, *114*, 10394.
(16) Wang, L.; Flood, T. C. *J. Am. Chem. Soc.* **1992**, *114*, 3169.
(17) Flood, T. C.; Bitler, S. P. *J. Am. Chem. Soc.* **1984**, *106*, 6076.
(18) Flood, T. C.; Statler, J. A. *Organometallics* **1984**, *3*, 1795.
(19) Ermer, S. P.; Struck, G. E.; Bitler, S. P.; Richards, R.; Bau, R.; Flood, T. C. *Organometallics* **1993**, *12*, 2634.
(20) Clark, H. C.; Jablonski, C. R.; Von Werner, K. *J. Organomet. Chem.* **1974**, *82*, C51.
(21) Cramer, R. *J. Am. Chem. Soc.* **1965**, *87*, 4717.
(22) Pardy, R. A. *J. Organomet. Chem.* **1981**, *216*, C29.
(23) Halpern, J.; Okamoto, T. *Inorg. Chim. Acta* **1984**, *89*, L53.
(24) Doherty, N. M.; Bercaw, J. E. *J. Am. Chem. Soc.* **1985**, *107*, 2670.
(25) Burger, B. J.; Santarsiero, B. D.; Trimmer, M. S.; Bercaw, J. E. *J. Am. Chem. Soc.* **1988**, *110*, 3134.

0002-7863/96/1518-2436$12.00/0

reactions and methods to control rates and selectivities in catalytic reactions involving such insertions. In this regard, we report here a study of the migratory insertion reactions of a series of *para*-substituted styrene alkyl Pd(II) complexes (1,10-phenanthroline)Pd(CH_3)(*p*-X-styrene)$^+$ (X = CF_3, Cl, H, CH_3, OCH_3). These complexes rearrange at low temperature by β-methyl migration to the CH_2 terminus of *p*-X-styrene, yielding a family of η^3-π-benzyl complexes, (phen)Pd(η^3-CH(CH_2CH_3)-C_6H_4-*p*-X)$^+$. In light of the importance of ground-state stabilities revealed in the studies of β-H-migratory insertion,[23−25] a combination of kinetic and thermodynamic studies were employed here to fully define the β-CH_3 migratory insertion reaction.

A β-H elimination reaction was discovered during the studies of the β-CH_3 migratory insertion. In the presence of excess styrene, the elimination of (*E*)-β-methylstyrene from the π-benzyl (phen)Pd(η^3-CH(CH_2CH_3)C_6H_5)$^+$ and formation of (phen)-Pd(η^3-CH(CH_3)C_6H_5)$^+$ occurs. We report here a detailed investigation, employing kinetic and isotopic labeling experiments, of the mechanism of this unusual benzyl transfer reaction.

Results and Discussion

1. Preparation and Characterization of (phen)Pd(CH_3)-(OEt_2)$^+$ (1). The cationic diethyl ether adduct (phen)Pd(CH_3)-(OEt_2)$^+$ (**1**) is a useful precursor to (phen)Pd(CH_3)(olefin)$^+$ complexes. Complex **1** is prepared by low-temperature (−30 °C) protonation of (phen)Pd(CH_3)$_2$ with $H^+(OEt_2)_2Ar'_4B^-$ in a $3CH_2Cl_2/1Et_2O$ (v/v) solvent pair. The pale yellow ether

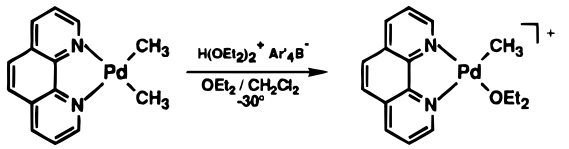

1 (3)

complex is thermally unstable in solution but is reasonably stable in the solid-state at room temperature. This requires that the protonation be undertaken in the correct amount of solvent for crystallization. After the protonation is complete, when the mostly insoluble orange (phen)Pd(CH_3)$_2$ is consumed, the reaction mixture is warmed only long enough to dissolve any precipitated product. Subsequent cooling from −30 to −78 °C over a period of hours produces crystalline **1**.

An X-ray quality crystal of **1** was grown from diffusion of a concentrated ether solution of **1** into hexane at room temperature (Figure 1, Table 1). Crystallization occurred rapidly. Although this was accompanied by some visible decomposition, it did not interfere with the low-temperature (−170 °C) X-ray analysis. This is a rare example of a crystallographically characterized organometallic ether adduct.[26] Two interesting features of the X-ray structure are the "upright" nature of the ether ligand and its widely different *trans*-effect compared to CH_3. The roughly perpendicular orientation of the ether ligand, with respect to phenanthroline, is reminiscent of the conformations adopted by olefin ligands coordinated to square planar Pd(II) or Pt(II) complexes; the upright geometry minimizes steric repulsions between the ether (or olefin) and the other members of the square plane.[27] Steric demands must also dictate the favorable *anti*-geometry of the ether backbone. Secondly, the expected variation in *trans* effects of OEt_2 and CH_3 is clearly demonstrated by the large difference between the two Pd−N bond lengths, the bond *trans* to CH_3 being *ca.* 0.1 Å longer than that *trans* to oxygen.

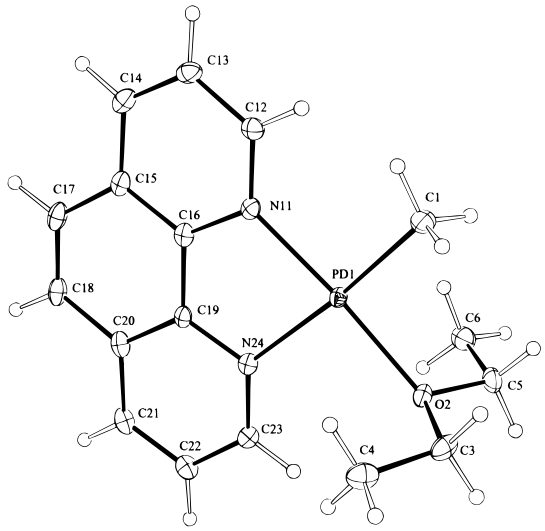

Figure 1. ORTEP structure of (phen)Pd(CH_3)(OEt_2)$^+$$Ar'_4B^-$ (**1**). The Ar'_4B^- counterion is not shown for the sake of clarity. All atoms are drawn at 50% probability ellipsoids except for hydrogens, which have been assigned arbitrary thermal parameters.

Table 1. Selected Bond Lengths (Å), Angles (deg), and Torsion Angles (deg) of (phen)Pd(CH_3)(OEt_2)$^+$$Ar'_4B^-$ (**1**)

Pd1−N11	2.0233(23)	Pd1−C1	2.024(3)
Pd1−N24	2.1271(24)	C4−O2	1.464(4)
Pd1−O2	2.0952(19)	C6−O2	1.458(4)
N11−Pd1−N24	81.05(09)	C2−Pd1−O2	92.10(11)
N11−Pd1−C1	94.17(12)	C5−C4−O2	109.11(24)
C4−O2−C6	112.85(22)	O2−C6−C12	109.23(24)
Pd1−O2−C3−C4	49.3(1)	N24−Pd1−O2−C3	−106.6(2)
C1−Pd1−O2−C3	73.8(2)	C1−Pd1−O2−C5	−65.4(2)
Pd1−O2−C5−C6	−43.0(1)		

Hindered rotation of the ether ligand around the Pd−O axis has been observed. As shown in the ORTEP drawing of **1**, the methylene hydrogens are diastereotopic and magnetically inequivalent. At −78 °C, these methylene protons exhibit two overlapping doublets of quartets due to coupling to geminal and methyl protons. Upon raising the temperature, rotation and inversion cause site exchange between the diastereotopic protons on opposite methylenes to occur; the two sets of multiplets coalesce at −52 °C. The exchange rate was estimated from the coalescence data to be $k = 73 \pm 15$ s^{-1}, $\Delta G^{\ddagger} = 10.9 \pm 0.3$ kcal/mol. Decoupling the methyl resonance reduced the methylene resonances to an AB pattern. The interconversion of these doublets at −61 °C was simulated using the DNMR3 program, giving a comparable activation energy, $k = 14 \pm 3$ s^{-1}, $\Delta G^{\ddagger} = 11.2 \pm 0.1$ kcal/mol. Only at a higher temperatures (−25 °C) was exchange with trace amounts of free ether observed in the ^{1}H NMR spectrum, confirming that the lower temperature process was not intermolecular Et_2O exchange.

2. Preparation and Characterization of (phen)Pd(CH_3)-(*p*-X-$C_6H_4CH{=}CH_2$)$^+$ (X = CF_3, Cl, H, CH_3, OCH_3) (2X). The coordinated ether ligand of **1** is quite labile. We have previously reported that substitution of Et_2O by ethylene or CO occurs rapidly at −78 °C.[11] The facile substitution of Et_2O by *para*-substituted styrenes is a convenient route to prepare cationic styrene complexes (phen)Pd(CH_3)(*p*-X-$C_6H_4CH{=}CH_2$)$^+$ (X = CF_3, Cl, H, CH_3, OCH_3) (eq 4). When slightly less than 1 equiv of styrene is added to **1** at −78 °C, (phen)Pd(CH_3)(C_6H_5-$CH{=}CH_2$)$^+$ (**2H**) is formed as a pair of rotamers in a 1.9:1

(26) Braunstein, P.; Knorr, M.; Tiripicchio, A.; Camellini, M. T. *Angew. Chem., Int. Ed. Engl.* **1989**, *28*, 1361.

(27) Albright, T. A.; Hoffmann, R.; Thibeault, J. C.; Thorn, D. L. *J. Am. Chem. Soc.* **1979**, *101*, 3801 and references therein.

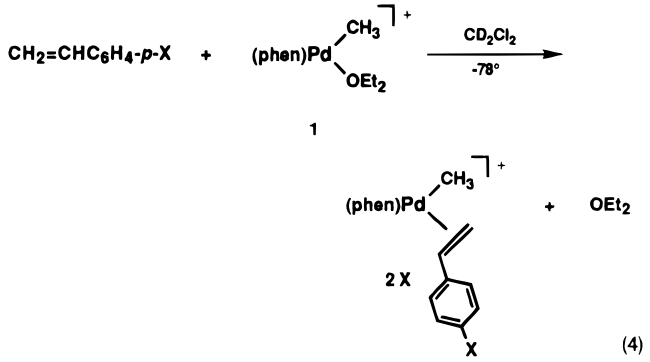

($\mathbf{2H}_{maj}$:$\mathbf{2H}_{min}$) ratio due to hindered rotation about the Pd-olefin axis (eq 5) at −95 °C. The populations and rates of intercon-

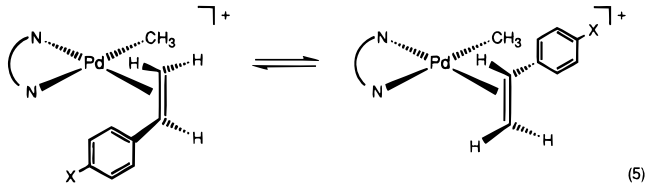

version of the rotamers are equivalent for *p*-H (1.9:1) and *p*-OCH_3 (2:1) styrene (*p*-H: $\Delta G^{\ddagger}_{min\rightarrow maj} = 10.2 \pm 0.1$ kcal/mol, $\Delta G^{\ddagger}_{maj\rightarrow min} = 10.5 \pm 0.1$ kcal/mol; *p*-OMe: $\Delta G^{\ddagger}_{min\rightarrow maj} = 10.3 \pm 0.1$ kcal/mol, $\Delta G^{\ddagger}_{maj\rightarrow min} = 10.5 \pm 0.1$ kcal/mol), indicating no electronic preference for either rotamer. The addition of 1.5 equiv of styrene to **1** yields a single set of resonances for **2H** in the ^{1}H and ^{13}C NMR spectra and only one set of resonances for both free and coordinated styrene at −80 °C. Thus, the presence of excess styrene acts to dramatically increase the rate of interconversion between $\mathbf{2H}_{maj}$ and $\mathbf{2H}_{min}$ by associative exchange between free and coordinated styrene. A similar effect was previously observed in the ethylene analogue of **2X**.[11]

The exact geometry of the two rotamers with respect to the other members of the square plane is not known. However, it is reasonable to assume that, as in crystallographically determined structures of square planar styrene complexes, the styrene is upright as is the ether in **1**.[27] This results in *endo* and *exo* (Ar relative to CH_3) isomers of styrene. The very high stretching frequency of the carbonyl analog of **1**, (phen)Pd(CH_3)(CO)$^+$, $\nu_{CO} = 2130$ cm^{-1},[11] indicates that very little back-bonding between Pd and CO is present.[28] This suggests that styrene binding in **3X** will be dominated by donation from the pπ orbital of styrene to palladium and that little back-bonding from dπ to pπ* will occur.

3. Investigation of the β-CH_3 Migratory Insertion Reaction of 2X. (a) Structural Characterization of the Insertion Product, (phen)Pd(*anti*-η^3-CH(CH_2CH_3)C_6H_5)$^+$ (3H). When a solution of **2H** is warmed to room temperature, it is transformed into a new species, **3H**, whose ^{1}H and ^{13}C NMR data identify it as the η^3-π-benzyl complex (phen)Pd(η^3-CH(CH_2CH_3)C_6H_5)$^+$ (eq 6). Key spectral features include the chemical shifts of the methine proton (δ 4.06, dd) and carbon (δ 65.7), as well as the ortho arene hydrogens (δ 7.29, 6.66) and carbons (δ 107.7, 105.3). Similar spectral features have been reported for other π-benzyl complexes[29−42] including

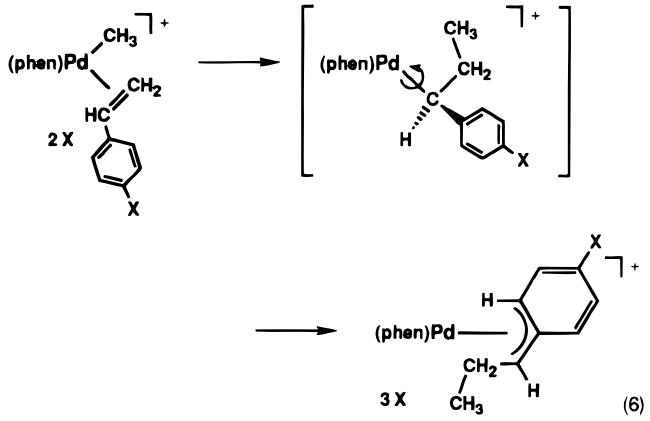

(bipy)Pd(η^3-CH($CH_2C(O)CH_3$)C_6H_4-*p*-tBu)$^+$.[43] A single crystal suitable for X-ray analysis was obtained from slow diffusion of a diethyl ether solution of **3H** into hexanes. An ORTEP drawing and key structural features of **3H** are presented in Figure 2. The structure confirms that **3H** is an η^3-π-benzyl complex and, therefore, that methyl migration occurs to the methylene carbon. The structure also reveals that the ethyl group adopts the *anti*-configuration in the solid-state. No syn isomer was observed by NMR spectroscopy at −78 °C. This is curious since the *syn*:*anti* ratio of the related η^3-π-allyl (phen)Pd(η^3-$CH_2CHCH(CH_3)$) is 9:1; the origin of this difference has been proposed, on the basis of molecular mechanics calculations, to arise from unfavorable interactions of the *anti*-methyl group and the phenanthroline.[44] In 1979, Maitlis and co-workers reported that extremely rapid suprafacial [1,5] palladium shifts caused site exchange between the ortho hydrogens of the π-benzyl (acac)Pd(η^3-C(C_6H_5)(C_6H_5)$_2$) ($\Delta G^{\ddagger} \sim 6.4$ kcal/mol, −86 °C).[33] Arene dissociation and rotation were also observed, but only at higher temperatures. A similar [1,5] rearrangement in **3H** would interconvert the *anti*- and *syn*-isomers. Therefore, it is possible that **3H** selectively crystallizes in the *anti*-configuration but, in solution, exists as a mixture of the two isomers, whose rapid interconversion causes a time-averaged spectrum to be observed.

(b) Dynamic Behavior of 3H. A dynamic process interconverts the protons on the two inequivalent sides of the phenyl ring without affecting the other resonances in the ^{1}H NMR spectrum (Scheme 1). This type of behavior, which cannot be *syn*,*anti* exchange, was first described by Cotton and Marks for $Cp(CO)_2Mo(\eta^3$-$CH_2C_6H_5)$ and explained in terms of an arene dissociation, arene rotation, arene reassociation mechanism analogous to the well-known $\eta^3-\eta^1-\eta^3$ allyl rearrangement.[34,35]

The rate of exchange of the *ortho* hydrogens of **3H** was measured at −2 °C using the spin saturation transfer technique, $k_{ex} = 0.6 \pm 0.1$ s^{-1}.[45,46] Interpretation of this rate constant depends upon whether or not the arene rotates freely in the η^1-

(28) Huang, L.; Ozawa, F.; Yamamoto, A. *Organometallics* **1990**, *9*, 2603.
(29) Stevens, R. R.; Shier, G. D. *J. Organomet. Chem.* **1970**, *21*, 495.
(30) Sonoda, A.; Mann, B. E.; Maitlis, P. M. *J. Chem. Soc., Chem. Commun.* **1975**, 108.
(31) Becker, Y.; Stille, J. K. *J. Am. Chem. Soc.* **1978**, *100*, 845.
(32) Roberts, J. S.; Klabunde, K. J. *J. Am. Chem. Soc.* **1977**, *99*, 2509.
(33) Mann, B.; Keasey, A.; Sonoda, A.; Maitlis, P. *J. Chem. Soc., Dalton Trans.* **1979**, 338.
(34) Cotton, F. A.; LaPrade, M. D. *J. Am. Chem. Soc.* **1968**, *90*, 5418.
(35) Cotton, F. A.; Marks, T. J. *J. Am. Chem. Soc.* **1969**, *91*, 1339.
(36) Galamb, V.; Pályi, G. *J. Chem. Soc., Chem. Commun.* **1982**, 487.
(37) Stühler, H. O. *Angew. Chem., Int. Ed. Engl.* **1980**, *19*, 468.
(38) Su, S.; Wojcicki, A. *Organometallics* **1983**, *2*, 1296.
(39) Carmona, E.; Marin, J. M.; Paneque, M.; Poveda, M. *Organometallics* **1987**, *6*, 1757.
(40) Mann, B. E.; Shaw, S. D. *J. Organomet. Chem.* **1987**, *326*, C13.
(41) Brookhart, M.; Buck, R. C.; Danielson, E., III. *J. Am. Chem. Soc.* **1989**, *111*, 567.
(42) Crascall, L. E.; Lister, S. A.; Redhouse, A. D.; Spencer, J. L. *J. Organomet. Chem.* **1990**, *394*, C35.
(43) Brookhart, M.; Rix, F. C.; DeSimone, J. M.; Barborak, J. C. *J. Am. Chem. Soc.* **1992**, *114*, 5894.
(44) Sjögren, M.; Hansson, S.; Norrby, P.-O.; Akermark, B.; Cucciolito, M. E.; Vitagliano, A. *Organometallics* **1992**, *11*, 3954.
(45) Forsén, S.; Hoffman, R. A. *J. Chem. Phys.* **1963**, *39*, 2892.

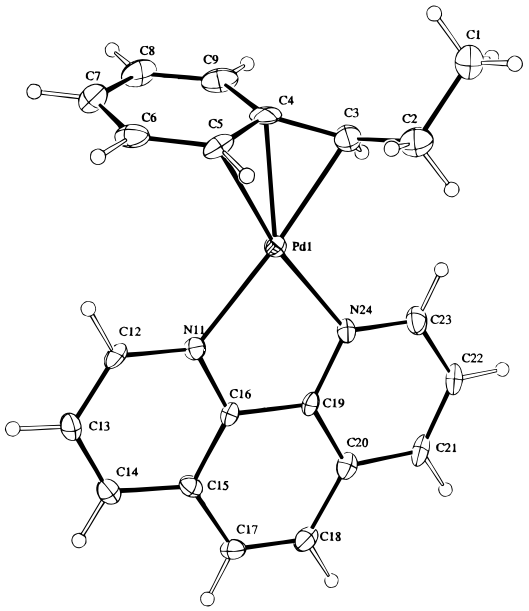

Figure 2. ORTEP structure of (phen)Pd(*anti*-η^3-CH(CH_2CH_3)C_6H_5)$^+$-Ar′$_4$B$^-$. The Ar′$_4$B$^-$ counterion is not shown for the sake of clarity. All atoms are drawn at 50% probability ellipsoids except for hydrogens, which have been assigned arbitrary thermal parameters.

Table 2. Selected Bond Lengths (Å) and Angles (deg) for (phen)Pd(η^3-CH(CH_2CH_3)C_6H_5)$^+$Ar′$_4$B$^-$ (**3H**)

Pd1−N11	2.139(07)	C4−C5	1.423(15)
Pd1−N24	2.096(07)	C9−C4	1.446(15)
Pd1−C3	2.117(10)	C5−C6	1.374(14)
Pd1−C4	2.135(09)	C6−C7	1.381(16)
Pd1−C5	2.251(09)	C7−C8	1.356(17)
C3−C4	1.403(14)	C8−C9	1.361(17)
N11−Pd1−N24	79.2(3)	C5−C4−C3	120.4(10)
C3−Pd1−N24	104.8(3)	C5−C4−C9	115.5(09)
C4−Pd1−N11	137.0(3)	C3−C4−C9	122.2(10)
C5−Pd1−N11	108.3(3)	C4−C9−C8	121.0(09)

benzyl intermediate. If it does, a factor of one-half must be applied to connect k_{ex} with the rate constant for for arene dissociation (k_{diss}), $k_{ex} = {}^1/_2 k_{diss}$, to account for the equal probability of either face of the arene coordinating from the η^1 intermediate. However, since arene rotation in the η^1 intermediate may be slow relative to the rate of collapse back to the η^3 structure, the observed barrier, $\Delta G^{\ddagger} = 12.2 \pm 0.1$ kcal/mol, more properly reflects only the upper limit for the barrier to arene dissociation.

A common dynamic process for unsaturated metal alkyl complexes is β-H elimination and readdition.[24,25,46−51] When combined with olefin rotation, which allows H migration to occur to either end of the olefin, "chain running" of the metal along the length of the alkyl ligand is observed.[8,13,52] This event is seen in the partially deuterium labeled complex (phen)Pd(η^3-CD(CD_2CH_3)C_6D_5)$^+$ (**3**-d_8). Complex **3**-d_8 was prepared *in situ* from 0.9 equiv of styrene-d_8 and **1** at *ca.* +5 °C, and the rearrangement was monitored at +25 °C by ^{2}H{^{1}H} NMR spectroscopy. H/D exchange occurred first between the methyl and methylene sites, followed by scrambling into the methine position until a statistical distribution of D in the three available sites was obtained.

A mechanism for the chain running process is shown in Scheme 2. Facile formation of the η^1-benzyl complex occurs upon arene dissociation, followed by β-D elimination from the CD_2 group, to form an (*Z*)- or (*E*)-β-methylstyrene deuteride complex (process **A**). Olefin rotation allows the Pd-D to migrate to either end of the olefin. Migration to the CDAr terminus places the CH_3 hydrogens in a β position (process **B**). β-H elimination generates a 3-phenyl-1-propene−hydride complex (process **C**). 3-Phenyl-1-propene rotation and β-H migration to the **C**DCD_2-carbon places a CHD group in the β position (process **D**). Now, either H or D may β-eliminate. These last two processes, **C** and **D**, scramble H and D between the methylene and methyl sites and must occur before processes **B** and **A** can bleed H into the methine position.

(c) Mechanistic Studies of the Reaction of (phen)Pd(η^3-CH(CH_2CH_3)C_6H_5)$^+$ (3H) and Styrene. The synthesis of **3H** revealed an interesting benzyl transfer reaction. When **1** reacts with excess styrene, the initial product **3H** reacts further with styrene to form a new π-benzyl complex, (phen)Pd(η^3-CH(CH_3)-C_6H_5)$^+$ (**4**) and (*E*)-β-methylstyrene.[53] The exchange reaction

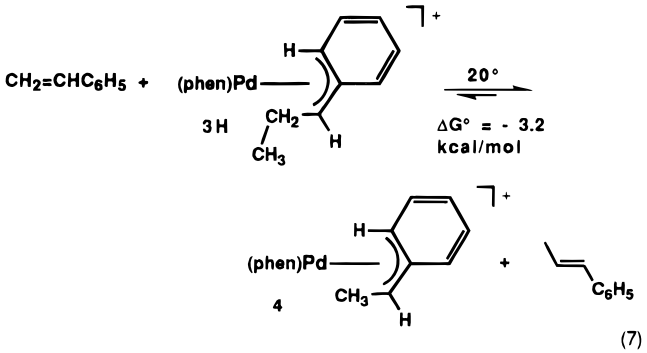

(7)

is reversible ($K_{eq} = 249 \pm 4$, $\Delta G° = 3.2$ kcal/mol) but lies heavily toward the right of eq 7 due, in part, to the stability of the disubstituted *trans*-olefin. This has allowed **4** to be isolated on a large scale. When the same reaction was carried out with 1 equiv of styrene-d_8 at 20 °C, the initial organometallic product was (phen)Pd(η^3-CD(CD_2H)C_6D_5)$^+$, which was subsequently equilibrated with (phen)Pd(η^3-CH(CD_3)C_6D_5)$^+$ upon scrambling of H into the methine position.

The benzyl transfer has been studied by a combination of kinetic and isotopic labeling experiments. The rate constants for the reaction were studied at −2 °C as a function of the concentrations of styrene and **3H**. A table of kinetic data is given in the Experimental Section (Table 8). As shown in the plot of $10^4\ k_{obsd}$ vs [styrene] in Figure 3, k_{obsd} does not increase linearly with [styrene] but begins to level off at high [styrene]. The maximum rate measured ($k = 5.4 \times 10^{-4}$ s^{-1}) corresponds to the largest practical amount of styrene (200 μL) that could be added to the 0.7 mL CD_2Cl_2 solution of **3H** ([styrene] = 1.84 M). The rate constant in the saturation limit was calculated from plots of $1/k_{obsd}$ vs 1/[styrene] for two concentrations of **3H** (0.0127 and 0.027 M) (Figure 3). The limiting rate constant, which is independent of [**3H**], was obtained from the average intercept (=$1/k_{lim}$) of these plots: $k_{lim} = (8.8 \pm 0.5) \times 10^{-4}$ s^{-1}, $\Delta G^{\ddagger} = 19.6 \pm 0.1$ kcal/mol.

(46) Cross, R. J. In *The Chemistry of the Metal−Carbon Bond*; Hartley, F. R., Patai, S., Eds.; Wiley: New York, 1985; Vol. 2, Chapter 8.
(47) Whitesides, G. M.; Gaasch, J. F.; Stedronsky, E. R. *J. Am. Chem. Soc.* **1972**, *94*, 5258.
(48) McDermott, J. X.; White, J. F.; Whitesides, G. M. *J. Am. Chem. Soc.* **1973**, *95*, 4451.
(49) McDermott, J. X.; White, J. F.; Whitesides, G. M. *J. Am. Chem. Soc.* **1976**, *98*, 6521.
(50) Ozawa, F.; Ito, T.; Yamamoto, A. *J. Am. Chem. Soc.* **1980**, *102*, 6457.
(51) Miller, T. M.; Whitesides, G. M. *Organometallics* **1986**, *5*, 1473.
(52) Brookhart, M.; Grant, B. E. *J. Am. Chem. Soc.* **1993**, *115*, 2151.
(53) Carr, N.; Mole, L.; Orpen, A. G.; Spencer, J. L. *J. Chem. Soc., Dalton Trans.* **1992**, 2653.

Scheme 1. $\eta^3-\eta^1-\eta^3$ Rearrangement Mechanism That Accounts for the Observed Exchange of the Ortho Hydrogens in the ^{1}H NMR Spectra of **3H**

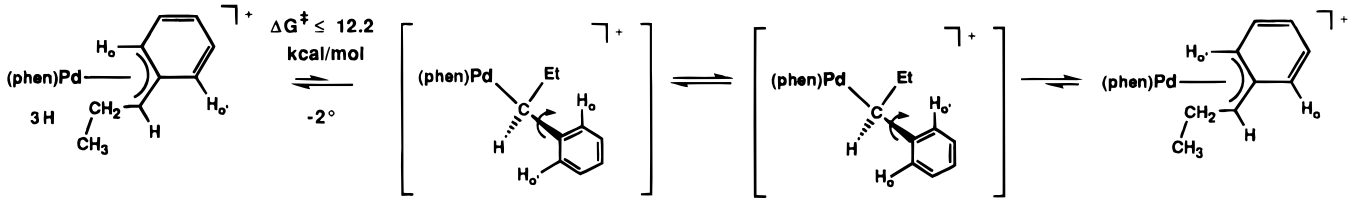

Scheme 2. Chain Running Mechanism for H/D Scrambling in (phen)Pd(η^3-CD(CD_2CH_3)C_6D_5)$^+$ (**3**-d_8)

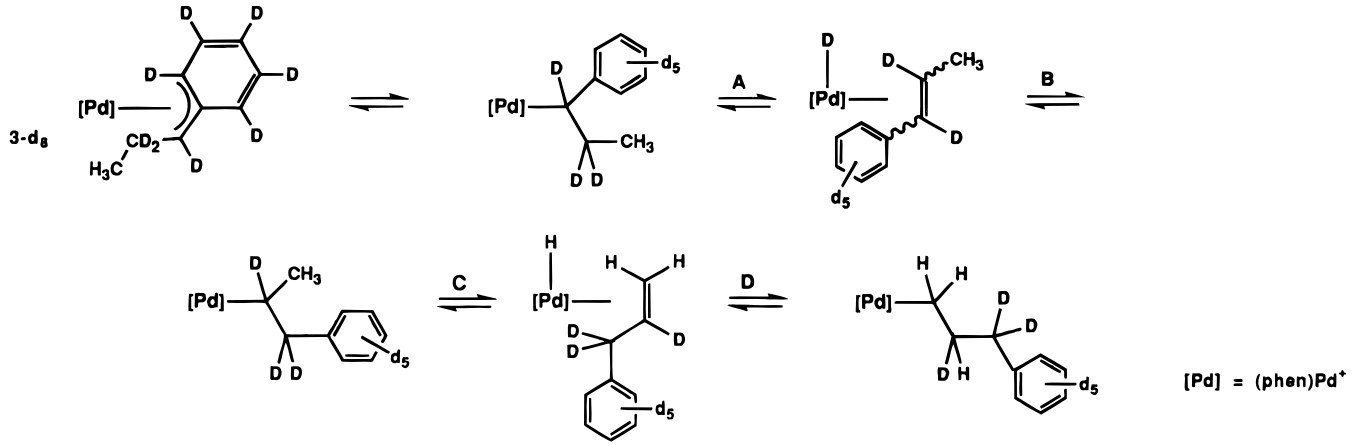

The two simplest mechanisms for the benzyl transfer involve β-H elimination but differ in the method of exchange of styrene for (*E*)-β-methylstyrene. If dissociation of (*E*)-β-methylstyrene was the rate-limiting step, the competition between (*E*)-β-methylstyrene and styrene for a palladium hydride intermediate would give rise to saturation kinetics at high [styrene]. This mechanism would agree with Spencer's report that the platinum π-benzyl complex (^{t}Bu$_2$P(CH$_2$)$_3$^{t}Bu$_2$)Pt(η^3-CH(CH$_3$)C_6H_5)$^+$ liberates styrene and forms the dicationic bridging dihydride dimer [(^{t}Bu$_2$P(CH$_2$)$_3$P^{t}Bu$_2$)Pt-μ-H]$_2^{2+}$ upon standing.[42] A double label crossover experiment was performed to test this mechanism. The deuterated complex (phen)Pd(η^3-CD(CD_2CD_3)C_6D_5)$^+$ was prepared from (phen)Pd(CD_3)(OEt_2)$^+$ and styrene-d_8. An isotopomer with ^{13}C (99%) incorporation in the methylene carbon, (phen)Pd(η^3-CH($^{13}CH_2CH_3$)C_6H_5)$^+$ was prepared from **1** and [β-^{13}C]styrene. These two complexes were combined in

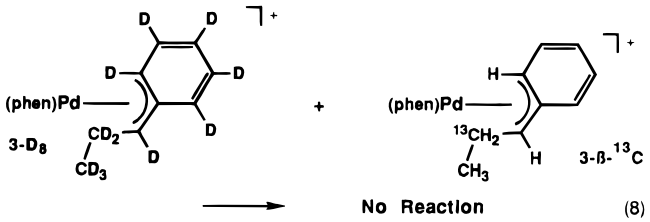

(8)

CD_2Cl_2 and monitored over the course of 1 week at 20 °C by ^{1}H and ^{13}C NMR spectroscopies. During this period, no $^{12}CH_nD_{2-n}$ (n = 1,2) appeared in the ^{1}H NMR spectrum and no $^1J_{CD}$ was observed in the $^{13}C\{^1H\}$ NMR spectrum, indicating that no crossover and thus no (*E*)-β-methylstyrene dissociation occurred.

The most reasonable mechanism for the benzyl transfer, accounting for the saturation kinetics and the negative crossover experiment, involves β-H elimination from the η^1-benzyl species as the rate-limiting step at high [styrene]. Note that the η^3 to η^1 conversion of the benzyl cannot be the rate-limiting step because it occurs at a much faster rate ($k_1 \geq 0.6 \pm 0.1$ s^{-1}) than the limiting rate of the benzyl exchange reaction (k_{lim} = ($(8.8 \pm 0.5) \times 10^{-4}$ s^{-1}). As shown in Scheme 4, β-H elimination from the η^1-benzyl **5** forms an η^2-(*E*)-β-methylstyrene hydride complex (**6**). A subsequent associative substitution of styrene for coordinated (*E*)-β-methylstyrene forms **7**, which rapidly rearranges initially to **8** upon β-H migration and finally to **4** with arene coordination to Pd.

A kinetic expression for the mechanism illustrated in Scheme 4 is obtained using steady-state approximations for the η^1-benzyl (**5**) and the (*E*)-β-methylstyrene hydride (**6**) intermediates. The kinetics are simplified by the approximation that styrene substitution for (*E*)-β-methylstyrene (**6** → **7**) is irreversible; the reverse reaction is certainly negligible over the time scale of the kinetics experiment since at 20 °C (*ca.* 20° higher in temperature) aproximately 1 day is required to attain equilibrium upon addition of 16 equiv of (*E*)-β-methylstyrene to **4**. Within these conditions, the kinetic expression is

$$-\mathrm{d}[\mathbf{3H}]/\mathrm{d}t = k_1k_2k_3[\mathbf{3H}][\text{styrene}]/(k_{-1}k_{-2} + (k_{-1} + k_2)k_3[\text{styrene}])$$

and thus,

$$k_{obsd} = k_1k_2k_3[\text{styrene}]/(k_{-1}k_{-2} + (k_{-1} + k_2)k_3[\text{styrene}])$$

In the limit where $(k_{-1} + k_2)k_3$[styrene] >> $k_{-1}k_{-2}$, the k_{obsd} becomes independent of [styrene]:

$$k_{lim} = k_{obsd} = k_1k_2/(k_{-1} + k_{-2})$$

The inverse plot, $1/k_{obsd}$ vs 1/[styrene] gives $1/k_{lim}$ as the intercept. The complete expression for $1/k_{obsd}$ is

$$1/k_{obsd} = \{(k_{-1}k_{-2})/(k_1k_2k_3)\}(1/[\text{styrene}]) + (k_{-1} + k_2)/(k_1k_2)$$

The slope and intercept of the line are the following ratios:

$$\text{slope} = (k_{-1}k_{-2})/(k_1k_2k_3)$$

$$\text{intercept} = (k_{-1} + k_{-2})/(k_1k_2) = 1/k_{lim}$$

The average slope and intercept of the two inverse plots yield

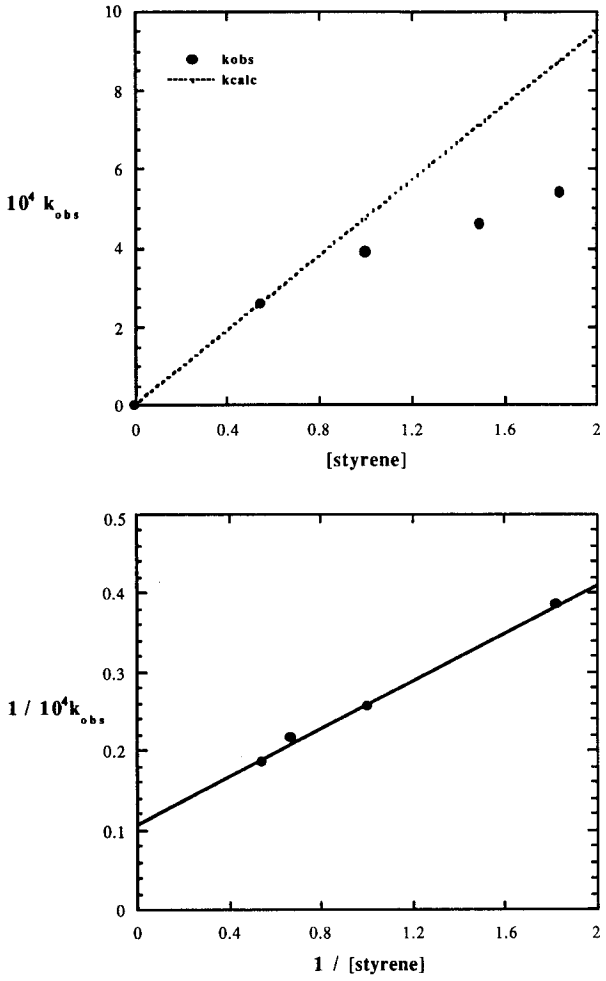

Figure 3. Representative kinetics plots for the reaction of (phen)Pd(η^3-CH(CH_2CH_3)C_6H_5)$^+$ (**3H**) ([**3H**] = 0.027 M) and styrene yielding (*E*)-β-methylstyrene and (phen)Pd(η^3-CH(CH_3)C_6H_5)$^+$ (**4**). The dashed line extrapolates k_{obsd} from [styrene] = 0 to the first point to illustrate the deviation of the plot from linearity. The k_{lim} was determined from the average intercept of the inverse plot, $k_{lim} = (8.8 \pm 0.5) \times 10^{-4}$ s^{-1}, $\Delta G^{\ddagger} = 19.6 \pm 0.1$ kcal/mol.

$$\text{slope} = (k_{-1}k_{-2})/(k_1k_2k_3) = (1.35 \pm 0.15) \times 10^3$$

$$\text{intercept} = (k_{-1} + k_2)/(k_1k_2) = 1/k_{lim} = (1.15 \pm 0.05) \times 10^3$$

The derived kinetics thus correctly predict saturation kinetics at high [styrene]. Also, this mechanism is supported by the extremely rapid associative styrene exchange observed for **2H** (section 2) and the H/D scrambling observed previously for (phen)Pd(η^3-CD(CD_2CH_3)C_6D_5)$^+$ (section 3b).

The associative olefin exchange mechanism and alkyl chain running (of **3**-d_3) may operate in other square-planar systems as well, including the closely related Pd-catalyzed isomerization of allylbenzene to β-methylstyrene.[54] Also, we have recently reported the dimerization of ethylene by (phen)Pd(CH_2CH_3)(C_2H_4)$^+$ to a mixture of butenes with the following percent composition: *trans*-2 > *cis*-2 > 1.[11] If a similar olefin substitution mechanism operates here, then ethylene displaces an η^2-butene of a (phen)Pd(butene)(H)$^+$ intermediate to restart the dimerization cycle. (The relative binding affinities of alkylolefins to Cp[(C_6H_5)$_3$P]Pd$^+$ are *trans* < *cis* < 1 < ethylene.[55]) Conversely, when the associative displacement of coordinated butene by ethylene is slow, as in the case of the sterically encumbered (ArN═C(R)C(R)═NAr)Pd(alkyl)(C_2H_4)$^+$Ar′$_4$B$^-$ (R = H, Me; Ar = 2,6-^{i}Pr$_2$$C_6H_3$) system, ethylene polymerization can result.[12]

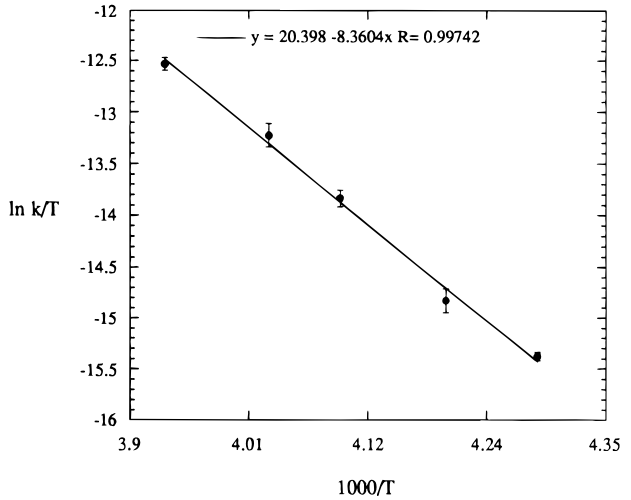

Figure 4. Eyring plot of the β-CH_3 migratory insertion reaction of (phen)Pd(CH_3)(C_6H_5CH═CH_2)$^+$ (**2H**) from −39.8 to −18.9 °C: $\Delta H^{\ddagger} = 16.6 \pm 1.3$ kcal/mol, $\Delta S^{\ddagger} = -6.7 \pm 5.4$ eu.

(d) Kinetic and Thermodynamic Studies of the β-CH_3 Migratory Insertion Reaction of 2X. The kinetics of the migratory insertion reaction of the unsubstituted styrene adduct **2H** to yield **3H** (eq 5) were studied by ^{1}H NMR spectroscopy between −40 and −19 °C (Figure 4, Table 3). Complex **2H** was prepared *in situ* from normally less than or equal to 1 equiv of styrene, allowing the rates of product formation to be uncomplicated by further reaction of **3H** with styrene during the kinetic studies and afterward when the reaction was warmed prior to obtaining an infinity point reading.

The presence of the two rotamers $\mathbf{2X}_{maj}$ and $\mathbf{2X}_{min}$ does not complicate the kinetic analysis since they are in very rapid equilibrium relative to the rate of migratory insertion and hence can be treated as a single species.

An Eyring plot for the migratory insertion of the styrene methyl complex has been constructed from five sets of averaged rate constants collected over a 21° (−39.8 to −18.9 °C) temperature range. It yields the activation parameters $\Delta H^{\ddagger} = 16.6 \pm 1.3$ kcal/mol and $\Delta S^{\ddagger} = -6.7 \pm 5.4$ eu. The entropy of activation is expected to be small on the basis of our earlier report that $\Delta S^{\ddagger} = -3.7 \pm 2.0$ eu for the β-ethyl migration of (phen)Pd(CH_2CH_3)(C_2H_4)$^+$ ($\Delta H^{\ddagger} = 18.5 \pm 0.6$ kcal/mol)[11] and other reports that $\Delta S^{\ddagger} \sim 0$ for β-alkyl and β-H migratory insertion reactions.[15,16,19,24,25] While there is substantial error in our $\Delta S^{\ddagger}$ determination, the value of -6.6 ± 5.4 eu is not inconsistent with an expected small $\Delta S^{\ddagger}$.

Electronic effects on the rate of β-CH_3 migratory insertion were probed by varying the *para*-substituent within a series of *p*-X-styrene (X = CF_3, Cl, H, CH_3, OCH_3) methyl complexes **2X** ((phen)Pd(CH_3)(*p*-X-C_6H_4CH═CH_2)$^+$). Averaged migratory insertion rate constants from two separate kinetic runs are reported in Table 3. Again, the presence of two rotamers for each complex does not complicate the kinetic analysis since rotamer interconversion is always much more rapid than methyl migration and the equilibrium ratio is insensitive to the *para*-substituent, X.

The data clearly indicate that the migratory insertion reaction is accelerated by electron-withdrawing substituents on the phenyl ring. Hammett plots of log *k* versus σ^p and σ^+ constants are shown in Figure 5. The data are fit only marginally better by σ^p ($\rho^p = 1.1 \pm 0.1$, $r = 0.991$) than by σ^+ ($\rho^+ = 0.67 \pm 0.1$,

(54) Cruikshank, B. I.; Davies, N. R. *Aust. J. Chem.* **1973**, *26*, 2635.
(55) Kurosawa, H.; Majima, T.; Asada, N. *J. Am. Chem. Soc.* **1980**, *102*, 6996.

Scheme 3. Possible Dissociative Mechanism for the Reaction of (phen)Pd(η^3-CH(CH$_2$CH$_3$)C$_6$H$_5$)$^+$ (**3H**) and Styrene ([Pd] = (phen)Pd$^+$)

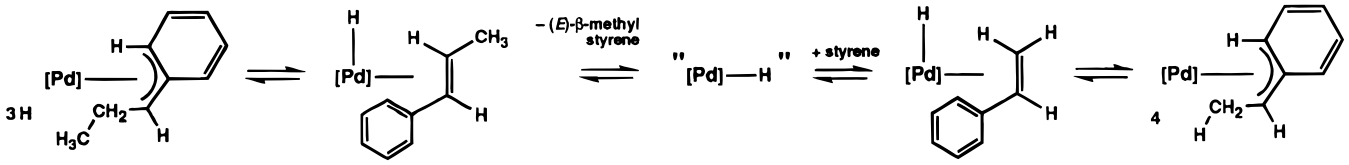

Scheme 4. Proposed Associative Benzyl Exchange Mechanism for the Reaction of (phen)Pd(η^3-CH(CH$_2$CH$_3$)C$_6$H$_5$)$^+$ (**3H**) and Styrene

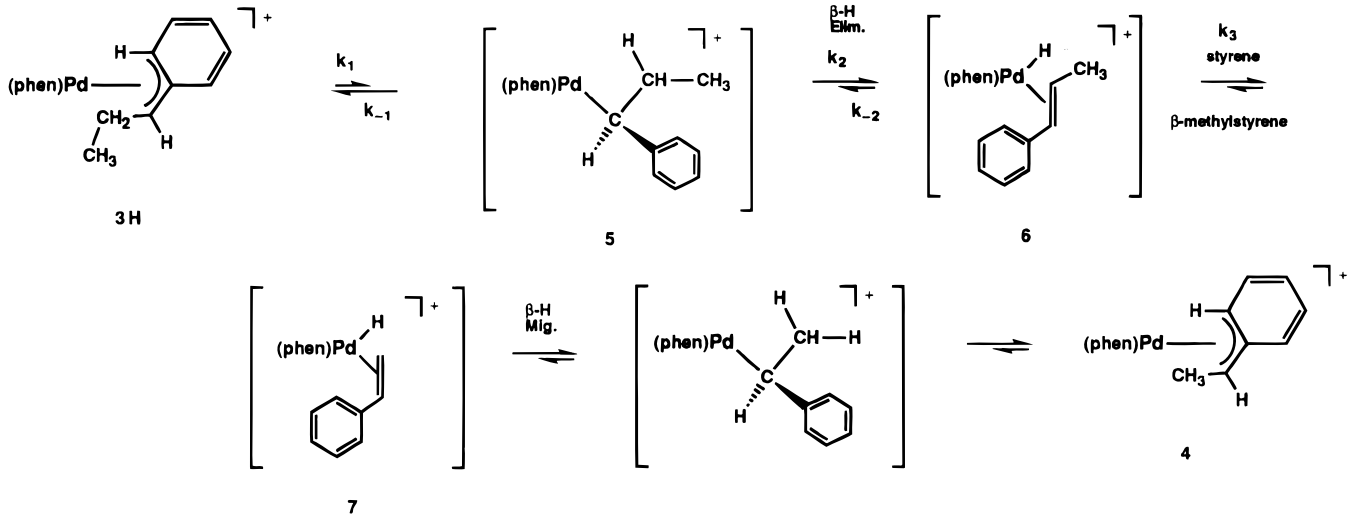

$r = 0.987$). The positive sign of the ρ indicates that the partial positive charge in the arene ring decreases in going from the ground-state π-complex to the transition state for migratory insertion.

To assess the role of the relative ground-state stabilities on the observed rate differences, the styrene binding affinities were determined. The equilibrium constants K_{AX} between the *para*-substituted styrenes and (phen)Pd(CH$_3$)(NCAr′)$^+$ (**9**) (Ar′- = 3,5-(CF$_3$)$_2$C$_6$H$_3$−), as shown in eq 9, were measured. Studies

$$\text{(phen)(CH}_3\text{)Pd(NCAr}')^+ + p\text{-}X\text{-styrene} \overset{K_{AX}}{\rightleftharpoons} \text{(phen)(CH}_3\text{)Pd(}p\text{-X-styrene)}^+ + \text{NCAr}' \quad (9)$$

were carried out at −66 °C to prevent interference from the migratory insertion reaction. The equilibrium constants are dependent upon *p*-X with the binding affinities decreasing in the order OCH$_3$ > CH$_3$ > H > Cl > CF$_3$. This behavior has also been reported by Kurosawa for several cationic palladium and platinum styrene complexes, including Cp(R$_3$P)Pd(*p*-Y-styrene)$^+$ and ((C$_6$H$_5$)$_3$P)(η^3-2-methallyl)M(*p*-Y-styrene)$^+$ (M = Pd, Pt).[55−61] The equilibrium constants for the exchange of

$$\text{(phen)(CH}_3\text{)Pd(styrene)}^+ + p\text{-X-styrene} \overset{K_{BX}}{\rightleftharpoons} \text{(phen)(CH}_3\text{)Pd(}p\text{-X-styrene)}^+ + \text{styrene} \quad (10)$$

p-X-styrene and styrene were calculated from $K_{BX} = K_{AX}/K_{AH}$. Hammett plots of K_{BX} (Figure 6) show that the data are fit quite well by σ ($\rho = -2.2 \pm 0.1$, $r = 0.999$) and satisfactorily by σ^+ ($\rho^+ = -1.3 \pm 0.1$, $r = 0.966$). The negative slopes of these Hammett plots are consistent with a partial positive charge developing on the π-bound *p*-X-styrene ligand upon coordination to the electrophilic cationic palladium center. Since the equilibrium constants K_{BX} are actually combined equilibrium constants for the two rotamers of **2X**, the linearity of the Hammett plot (σ^p) reveals that both rotamers are stabilized identically by X; this is consistent with the fact that rotamer ratios are independent of the identity of X.

Table 3. Rate Constants and Free Energies of Activation for β-CH$_3$ Migratory Insertion of **2X**

T (°C)	X	$10^4\,k$ (s^{-1})	$\Delta G^‡$ (kcal/mol)	$\Delta\Delta G^‡$ (kcal/mol)
−29.2	*p*-CF$_3$	8.8 ± 2.8	17.6 ± 0.1	−0.6 ± 0.2
−29.2	*p*-Cl	3.8 ± 0.6	18.0 ± 0.1	−0.2 ± 0.2
−29.2	*p*-H	2.4 ± 0.2	18.2 ± 0.1	0
−29.2	*p*-CH$_3$	1.8 ± 0.01	18.4 ± 0.1	+0.2 ± 0.2
−29.2	*p*-OCH$_3$	0.99 ± 0.23	18.7 ± 0.1	+0.5 ± 0.2
−39.8	*p*-H	0.49 ± 0.02	18.1 ± 0.1	
−35.0	*p*-H	0.87 ± 0.1	18.3 ± 0.1	
−25.1	*p*-H	4.5 ± 0.5	18.2 ± 0.1	
−18.9	*p*-H	9.2 ± 0.6	18.3 ± 0.1	

The relative transition-state energies are given by $\Delta G°_X + \Delta\Delta G^‡_X$ and are tabulated in Table 5 together with $\Delta G°_X$ and $\Delta\Delta G^‡_X$ values. There is substantial error in these transition state differences, but the basic trend is clear. *The same sensitivity to substituents is observed for the transition states as for the ground states (electron-donating substituents stabilize the transition state), but the magnitude of the sensitivity to the substituents is significantly less in the transition state.* Thus, electron-donating substituents also stabilize the transition-state but to a significantly lesser degree than the ground-state. For example, for the two extremes (*p*-OCH$_3$ and *p*-CF$_3$), a $\Delta G°_X$ difference of 1.7 kcal/mol is seen while the transition-state energies differ by only ca. 0.6 kcal/mol. A Hammett plot

(56) Ban, E.; Hughes, R. P.; Powell, J. *J. Organomet. Chem.* **1974**, *69*, 455.
(57) Kurosawa, H.; Asada, N. *J. Organomet. Chem.* **1981**, *217*, 259.
(58) Kurosawa, H.; Asada, N. *Organometallics* **1983**, *2*, 251.
(59) Miki, K.; Shiotani, O.; Kai, Y.; Kasai, N.; Kanatani, H.; Kurosawa, H. *Organometallics* **1983**, *2*, 585.
(60) Miki, K.; Yamatoya, K.; Kasai, N.; Kurosawa, H.; Urabe, A.; Emoto, M.; Tatsumi, K.; Nakamura, A. *J. Am. Chem. Soc.* **1988**, *110*, 3191.
(61) Nyburg, S. C.; Simpson, K.; Wong-Ng, W. *J. Chem. Soc., Dalton Trans.* **1976**, 1865.

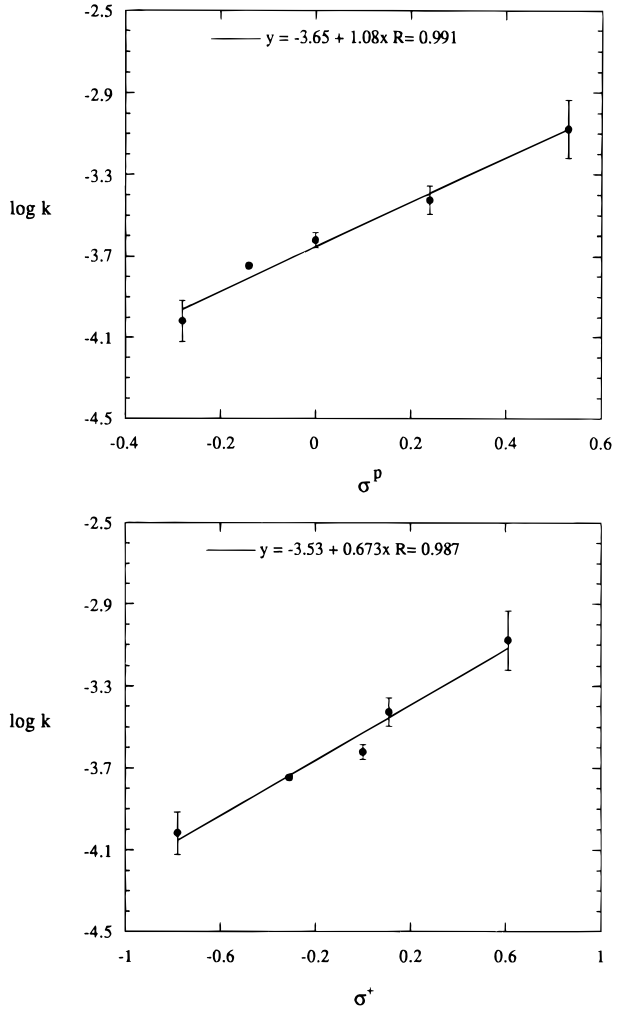

Figure 5. Hammett plots of the β-CH_3 migratory insertion of (phen)Pd(CH_3)(*p*-X-$C_6H_4CH{=}CH_2$)$^+$ at −29.2 °C. Slopes (ρ) have errors of ±0.1

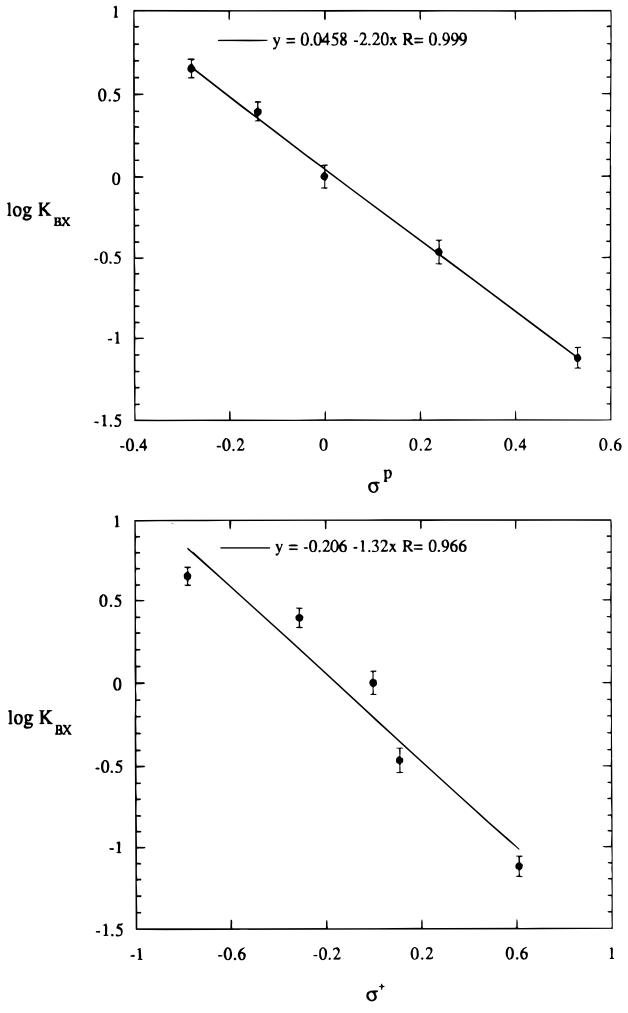

Figure 6. Hammett plots of the equilibria (phen)(CH_3)Pd(styrene)$^+$ + *p*-X-styrene $\overset{K_{BX}}{\rightleftharpoons}$ (phen)(CH_3)Pd(*p*-X-styrene)$^+$ + styrene. Slopes (ρ) have errors of ± 0.1.

created with the transition-state orderings ($-(\Delta G°_X + \Delta\Delta G_X^{\ddagger})$/2.30*RT*) gives an expected smaller $\rho^p = -0.76 \pm 0.3$ ($r = 0.97$). The most conservative assessment is, even with the significant errors associated with the transition-state orderings, that there is simply a decreased positive charge felt by the aryl substituent in the transition state, **10X**, relative to the ground state as depicted qualitatively in eq 11.

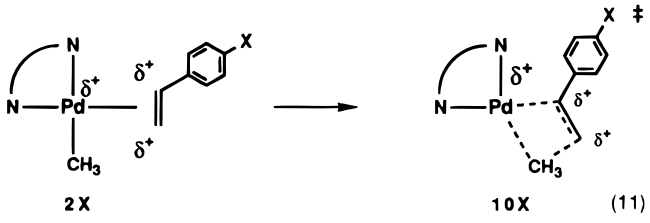

(11)

The structural basis for these results arises from the changing nature of the palladium−styrene bond upon moving from the ground state to the transition state. There is very little back-bonding in (phen)Pd(CH_3)(L)$^+$ between palladium and coordinated π-acids, L, such as CO (ν_{CO} = 2130 cm^{-1}) and *p*-X-styrene. The bonding between styrene and palladium is dominated by olefin π-donation to the metal. The polarization of the π-bond of the coordinated olefin induces a positive charge on the olefinic carbons felt by the *para*-substituted aryl ring. The ground-state orderings simply reflect the differing abilities of the substituted aryl groups to stabilize the induced dipole of the coordinated π-bond. Upon moving to the transition state, **10X**, the olefin π-electrons are partially transformed into σ-bonds, which are less polarizable than the dative olefin

Table 4. Equilibrium Constants for (phen)(CH_3)Pd(NCAr′)$^+$ + *p*-X-Styrene $\overset{K_{AX}}{\rightleftharpoons}$ (phen)(CH_3)Pd(*p*-X-styrene)$^+$ + NCAr′ and (phen)(CH_3)Pd(styrene)$^+$ + *p*-X-Styrene $\overset{K_{BX}}{\rightleftharpoons}$ (phen)(CH_3)Pd(*p*-X-styrene)$^+$ + Styrene

X	$10^3 K_{AX}$	$K_{BX} = K_{AX}/K_{AH}$	$\Delta G°_X$[a,b] (kcal/mol)
p-CF_3	9.59 ± 0.69	0.0767 ± 0.011	1.1
p-Cl	43.4 ± 3.8	0.347 ± 0.058	0.43
p-H	125 ± 10	1 ± 0.16	0
p-CH_3	312 ± 18	2.50 ± 0.34	−0.38
p-OCH_3	565 ± 27	4.52 ± 0.58	−0.62

[a] $\Delta G°_X = \Delta G°_{BX}$. [b] ±0.05 kcal/mol.

Table 5. Comparison of Kinetic and Thermodynamic Parameters of the β-CH_3 Migratory Insertion Reaction of (phen)Pd(CH_3)(*p*-X-$C_6H_4CH{=}CH_2$)$^+$

X	$\Delta G°_X$	$\Delta\Delta G_X^{\ddagger}$	$\Delta G°_X + \Delta\Delta G_X^{\ddagger}$[a]
CF_3	1.1 ± 0.05	−0.6 ± 0.2	0.5 ± 0.25
Cl	0.43 ± 0.05	−0.2 ± 0.2	0.23 ± 0.25
H	0 ± 0.05	0 ± 0.2	0 ± 0.25
CH_3	−0.38 ± 0.05	+0.2 ± 0.2	−0.18 ± 0.25
OCH_3	−0.62 ± 0.05	+0.5 ± 0.2	−0.12 ± 0.25

[a] $\Delta G_X° + \Delta\Delta G_X^{\ddagger}$ = the difference in transition-state energies.

π-bond. Hence the positive charge of the complex is not as effectively transmitted to the aryl ring in the transition state as it is in the ground state. This relative effect gives rise to the positive ρ seen in the kinetic Hammett plots.

It is instructive to compare the results obtained here to those obtained by Bercaw[24,25] for the reversible β-H migratory insertions of *exo*- and *endo*-$Cp_2Nb(p\text{-}X\text{-}C_6H_4CH{=}CH_2)(H)$ complexes **11**-*endo* and **11**-*exo*:

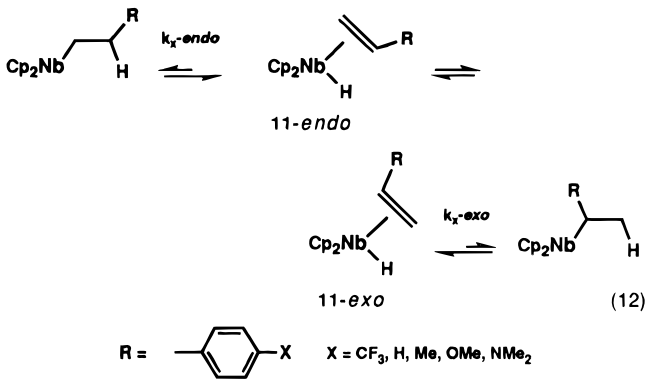

(12)

The *exo* and *endo* isomers are of approximately equal energy. Competitive binding experiments showed that electron-withdrawing substituents stabilize the ground state, suggesting that the $d\pi \rightarrow p\pi^*$ donation dominates the bonding interaction between Nb and the styrenes. A Hammett plot of the log of the relative binding constants, K_X, versus σ^p constants yield a ρ^p value of + 2.2 for **11**. These observations are consistent with the electron-rich nature of the d^2-niobium center and are in contrast to the cationic, electrophilic Pd(II) systems studied here where electron-donating substituents stabilize the η^2-styrene complex.

The relative rates of migratory insertion of the niobium *endo* isomers, k_X-*endo* are controlled by the relative differences in stabilities of the ground and transition states. A plot of log k_X-*endo* versus σ^p constants yielded $\rho^p = -1.06$, which indicates that the relative energies of the transition states are less sensitive to variations in X than are the η^2-styrene ground-state complexes, **11**. In contrast, the migratory insertion rates of the *exo*-isomers (which exhibit the same regiochemistry as the Pd systems studied here) are *accelerated* by electron-withdrawing substituents. A log k_X-*exo* versus σ^p plot yielded $\rho^p = +0.72$. This reversal of the direction of the substituent effects for k_X-*endo* vs k_X-*exo* must occur because the relative transition-state energies are now more sensitive to substituent variations than are the relative ground-state energies. Indeed, Bercaw showed that extraction of relative transition-state energies and construction of σ^p correlation plot yields $\rho^p = +2.8$ in comparison to $\rho^p = +2.2$ for correlation of relative ground-state energies. Thus a quantitative analysis of substituent effects on the rates of β-migratory insertion of *exo*-$Cp_2Nb(p\text{-}X\text{-}C_6H_4CH{=}CH_2)(H)$, **11**-*exo*, and $(phen)Pd(p\text{-}X\text{-}C_6H_4CH{=}CH_2)(CH_3)^+$ **2X**, yield similar results, $\rho^p = +0.72$ for **11**-*exo* and $\rho^p = +1.1$ for **2X**, but for very different reasons. In the case of **2X**, ground-state stabilities dominate and for these cationic Pd(II) systems, where back-bonding is negligible, the donor abilities of the styrenes dictate the relative ground-state stabilities. In the case of the niobium systems, **11**, the relative ground-state stabilities are controlled by the acceptor abilities of the styrenes. However, the relative rates of **11**-*exo* are now determined by relative transition-state stabilities. These transition states, like the ground-states, are stabilized by electron-withdrawing aryl groups but to an even greater extent.

Halpern has measured the values of K_{eq} for competitive binding of substituted styrenes and PPh_3 to the Rh(III) center in the complexes shown in eq 13.[23] Styrenes containing

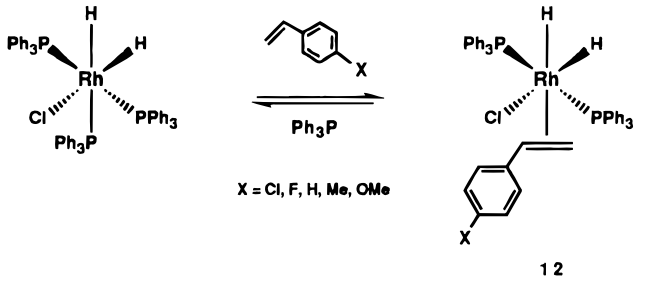

(13)

electron-withdrawing substituents exhibit greater binding affinities and a plot of log $K_{eq}(x)$ versus σ^+ values yields $\rho^+ =$ *ca.* 1 (eq 13). As in the niobium case, the dominant bonding mode between the styrenes and the rhodium center was suggested to be a $d\pi \rightarrow p\pi^*$ interaction. The rates of migratory insertion of **12** closely correlate with the ground-state stabilities; a plot of log $k_{ins}(x)$ versus σ^+ values yields ρ^+ of *ca.* -0.9. This case is analogous to the case of the *endo*-niobium system, **11**-*endo*, studied by Bercaw; however, the regiochemistry of the insertion of **12** is unknown.

Conclusions

A series of electrophilic $(phen)Pd(CH_3)(p\text{-}X\text{-}C_6H_4CH{=}CH_2)^+$ (**2X**) (X = CF_3, Cl, H, CH_3, OCH_3) complexes have been prepared. They rearrange at low temperature to η^3-π-benzyl complexes, $(phen)Pd(\eta^3\text{-}CH(CH_2CH_3)C_6H_4\text{-}p\text{-}X)^+$ (**3X**). The rates of migratory insertion of complex **2X** and the relative binding affinities of the *p*-X-styrene derivatives were compared to better understand the β-CH_3 migratory insertion reaction. There is a good correlation between the relative free energies of activation ($\Delta\Delta G^{\ddagger}$ values) and the relative binding affinities of the substituted styrenes, which supports the conclusion that the relative rates of the migratory insertion reactions of the *p*-X-styrene complexes are controlled primarily by their relative ground-state energy differences.

The reactivity and dynamic behavior of the parent $(phen)Pd(\eta^3\text{-}CH(CH_2CH_3)C_6H_4\text{-}p\text{-}H)^+$ (**3H**) have been investigated. The η^3 complex is in rapid equilibrium with its higher energy η^1-benzyl isomer which can undergo arene rotation and also "chain run" via multiple reversible β-H elimination, olefin rotation, and β-H migration steps along the length of the alkyl chain. Styrene reacts with **3H** to form free (*E*)-β-methylstyrene and a new π-benzyl complex, $(phen)Pd(\eta^3\text{-}CH(CH_3)C_6H_4\text{-}p\text{-}H)^+$. At high [styrene], this exchange proceeds by rate-limiting formation of $(phen)Pd((E)\text{-}CH_3CH{=}CHC_6H_5)(H)^+$, followed by associative styrene substitution of the coordinated olefin; β-H migration to styrene forms the new π-benzyl complex.

Experimental Section

General Methods. All reactions, except where indicated, were carried out in flame-dried glassware under a dry, oxygen-free argon atmosphere using a standard Schlenk line and drybox techniques. Non-deuterated solvents were distilled under a nitrogen atmosphere from a drying agent immediately prior to use: CH_2Cl_2 from P_4O_{10}; hexanes and diethyl ether from sodium benzophenone ketyl. CD_2Cl_2 was dried over CaH_2, submitted to five freeze−pump−thaw cycles, vacuum transferred into glass Schlenk tubes fitted with Kontes high-vacuum Teflon plugs, and stored under argon. *p*-Methoxystyrene was prepared from the parent aldehyde via a Wittig reaction by Mr. Delwin Elder of this laboratory. Styrene-d_8 and [β-^{13}C]styrene were purchased from

Cambridge Isotope Laboratories. $H^+(OEt_2)_2Ar'_4B^-$ [62] and (*N,N,N′,N′*-tetramethylethylenediamine)Pd$(CH_3)_2$[63] were prepared according to literature procedures.

NMR probe temperatures were measured using an anhydrous methanol sample. ^{1}H and ^{13}C chemical shifts were referenced to residual ^{1}H signals and to the ^{13}C signals of the deuterated solvents, respectively.

Atom labeling schemes for the phenanthroline and $((CF_3)_2C_6H_3)_4B^-$ counterion resonances are as follows:

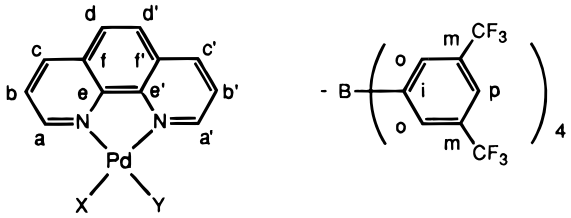

The ^{1}H NMR resonances were assigned into groups of a, b, c or a′, b′, c′ or d, d′ according to their characteristic coupling patterns. The ^{13}C NMR resonances were assigned in pairs such as C_a or $C_{a'}$ and $C_{a'}$ or C_a on the basis of their chemical shifts and $^1J_{CH}$. The relation between the ^{1}H and ^{13}C assignments and the stereochemistry with respect to the ligands X,Y has not been ascertained.

Activation parameters were calculated using the Eyring equation. The error analysis of the activation parameters was based on the derivation of $\sigma\Delta H^{\ddagger}$ and $\sigma\Delta S^{\ddagger}$ by Girolami and co-workers.[64] Error calculations for $\Delta G^{\ddagger}$ of DNMR processes, based on Binsch's derivation[65] of $\sigma\Delta G^{\ddagger}$, incorporated an estimate of 20% error in rate and a $\pm 1°$ error in temperature, except for coalescence data, which also incorporated a generous $\pm 5°$ error in the coalescence temperature, except where indicated.

Values for σ^+ and σ^p were taken from March's text;[66] with the exception of $\sigma^+(CF_3)$, which, not given by March, was taken from Hammett's text.[67] Uncertainties in the slopes of the Hammett plots were calculated by the standard method.[68]

C,H,N analyses were performed by Oneida Research Laboratories of Whitesboro, NY.

Synthesis of (1,10-Phenanthroline)Pd$(CH_3)_2$. This synthesis is a modified version of one previously reported by Boersma and co-workers for (2,2′-bipyridine)Pd$(CH_3)_2$;[63] the spectral characteristics of (phen)-Pd$(CH_3)_2$ were identical to those reported by Byers and Canty.[69] 1,-10-Phenanthroline·1H_2O (2.2 g, 11.1 × 10^{-3} mol) and degassed nondried acetone (20 mL) was slowly cannulated on top of a solution of (*N,N,N′,N′*-tetramethylethylenediamine)Pd$(CH_3)_2$ (2.0 g, 7.9 × 10^{-3} mol) and acetone (10 mL). Orange needles started to form at the interface of the two solutions after 15 min. After sitting undisturbed for *ca.* 1 day at 20 °C, the mother liquor was removed. The crystals were washed with Et_2O (2 × 20 mL) and then dried *in vacuo* to give (1,10-phenanthroline)Pd$(CH_3)_2$ (2.3 g, 92%) with spectral characteristics identical with those reported in the literature. Best results were obtained in the succeeding syntheses when this precursor was stored at −30 °C until needed.

Synthesis of (1,10-Phenanthroline)Pd$(CH_3)(OEt_2)^+Ar'_4B^-$ (1). Et_2O (0.5 mL) and CH_2Cl_2 (1.5 mL) was syringed onto (phen)Pd$(CH_3)_2$ (148 mg, 4.67 × 10^{-4} mol) and $H^+(OEt_2)_2Ar'_4B^-$ (505 mg, 4.99 × 10^{-4} mol) at −30 °C. After stirring at −30 °C for 2 h, the mixture was warmed briefly to dissolve the solid. The clear yellow solution was cooled to −30 °C; crystals appeared within 30 min. Slow cooling from −30 to −78 °C gave pale yellow crystals which, after cannulating off the mother liquor, washing with hexanes (2 × 10 mL), and drying *in vacuo*, were isolated as **1** (442 mg, 76%). It is important to remove all of the CH_2Cl_2 present since it induces decomposition of **1** in the solid state. Complex **1** is stable over a period of months when stored at −30 °C. Crystals suitable for X-ray diffraction were grown by diffusion of an Et_2O solution of **1** into hexane at 20 °C; this was accompanied by visible decomposition. The mother liquor was removed rapidly, and the crystals stored at −30 °C until the X-ray analysis was undertaken. Anal. Calcd for $C_{49}H_{39}BF_{24}N_2OPd$: C, 47.27; H, 3.16; N, 2.25. Found: C, 47.31; H, 2.68; N, 2.11.

^{1}H NMR (300.13 MHz, CD_2Cl_2, −80 °C): δ 8.71 (dd, J_{ab} = 5.31 Hz, J_{ac} = 1.06 Hz, 1H, H_a), 8.66 (dd, $J_{a'b'}$ = 4.84 Hz, $J_{a'c'}$ = 1.27 Hz, 1H, $H_{a'}$), 8.53 (dd, J_{bc} = 8.20 Hz, J_{ac} = 1.06 Hz, 1H, H_c), 8.47 (dd, $J_{b'c'}$ = 8.27 Hz, $J_{a'c'}$ = 1.27 Hz, 1H, $H_{c'}$), 7.95 (d, $J_{dd'}$ = 8.92 Hz, 1H, H_d or $H_{d'}$), 7.91 (d, $J_{dd'}$ = 8.92 Hz, 1H, $H_{d'}$ or H_d), 7.87 (dd, $J_{b'c'}$ = 8.27 Hz, $J_{a'b'}$ = 4.84 Hz, 1H, $H_{b'}$), 7.81 (dd, J_{bc} = 8.20 Hz, J_{ab} = 5.31 Hz, 1H, H_b), 7.73 (s, 8H, Ar′-H_o), 7.50 (s, 4H, Ar′-H_p), 3.88 (dq, $^2J_{AB}$ = 9.55 Hz, $^3J_{HH}$ = 6.8Hz, 2H, $H_AH_BCOCH_{A'}H_{B'}$), 3.77 (dq, $^2J_{AB}$ = 9.55 Hz, $^3J_{HH}$ = 6.8 Hz, 2H, $H_AH_BCOCH_{A'}H_{B'}$), 1.67 (t, J = 6.8 Hz, 6H, Et_2O CH_3), 0.93 (s, 3H, PdCH_3).

^{13}C NMR (75.4 MHz, CD_2Cl_2, −80 °C): δ 161.4 (q, $^1J_{CB}$ = 51 Hz, Ar′-C_i), 149.6 (d, J_{CH} = 186 Hz, C_a or $C_{a'}$), 147.1 (s, C_e or $C_{e'}$), 146.9 (d, J_{CH} = 184 Hz, $C_{a'}$ or C_a), 143.1 (s, $C_{e'}$ or C_e), 139.2 (d, J_{CH} = 167 Hz, C_c or $C_{c'}$), 138.4 (d, J_{CH} = 167 Hz, $C_{c'}$ or C_c), 134.2 (d, J_{CH} = 159 Hz, Ar′-C_o), 130.0 (s, C_f or $C_{f'}$), 129.3 (s, $C_{f'}$ or C $_f$), 128.2 (q, $^2J_{CF}$ = 31 Hz, Ar′-C_m), 127.2 (d, J_{CH} = 167 Hz, C_d or $C_{d'}$), 126.9 (d, J_{CH} = 168 Hz, $C_{d'}$ or C_d), 125.6 (d, J_{CH} = 167 Hz, C_b or $C_{b'}$), 125.0 (d, J_{CH} = 170 Hz, $C_{b'}$ or C_b), 123.9 (q, $^1J_{CF}$ = 273 Hz, Ar′-CF_3), 117.1 (d, J_{CH} = 165 Hz, Ar′-C_p), 72.48 (t, J_{CH} = 147 Hz, Et_2O CH_2), 16.1 (q, J_{CH} = 128 Hz, Et_2O CH_3), 2.50 (q, J_{CH} = 133 Hz, Pd-CH_3).

Determination of the Rate of Rotation of Diethyl Ether in 1. A 5 mm thin-walled NMR tube was charged with **1** (10 mg, 8.0 × 10^{-6} mol) in the drybox. CD_2Cl_2 (0.7 mL) was added at −78 °C; the sample was warmed briefly to dissolve **1** and placed in a precooled NMR probe (300 MHz, −80 °C). The two methylene multiplets coalesced at −52 °C, $k = 73 \pm 15$ s^{-1}, $\Delta G^{\ddagger} = 10.9 \pm 0.3$ kcal/mol. The exchange was also studied by decoupling the methyl resonance and modeling the interconversion of the resulting AB doublets with the dynamic NMR simulation program DNMR3. In this manner, the rate constant for rotation was determined at −61 °C to be $k = 14 \pm 3$ s^{-1}, $\Delta G^{\ddagger}$= 11.2 ± 0.1 kcal/mol, in agreement with the coalescence results. At a higher temperature, −25 °C, exchange with traces of free Et_2O began to contribute to line broadening of the methylene resonances.

Reaction of 1 with Styrene at Low Temperature. (a) Generation of (1,10-Phenanthroline)Pd$(CH_3)(\eta^2$-CH_2═C(H)$C_6H_5)$ (2H) from <1 Equiv of Styrene. A 5 mm NMR tube was charged with **1** (10 mg, 8 × 10^{-6} mol). CD_2Cl_2 (0.7 mL) was added at −78 °C, and the sample warmed briefly to dissolve **1**. Styrene (0.9 μL, 0.9 equiv) was added at −78 °C. The sample was placed in a precooled NMR probe (−84 °C). Two isomers were observed in a 1.9:1 ratio.

^{1}H NMR (300 MHz, CD_2Cl_2, −84 °C) (M = major isomer, m = minor isomer, ***M*** = M and m are overlapped, labeling scheme in Table 11): δ 9.0−7.3 (phen, Ar′, C_6H_5), 7.17 (dd, J_{trans} = 15 Hz, J_{cis} = 9 Hz, M-H_g), 7.0 (dd, J_{trans} = 15 Hz, J_{cis} = 9 Hz, m-H_g), 5.21 (d, J_{trans} = 15 Hz, m-H_c), 5.13 (d, J_{cis} = 15 Hz, M-H_c), 5.12 (d, J_{cis} = 9 Hz, M-H_t), 4.72 (d, J_{cis} = 9 Hz, m-H_t), 1.20 (s, m-CH_3), 0.59 (s, M-CH_3). The aromatic region is a complex series of bands due to the presence of phenanthroline, counterion and phenyl resonances of the two complexes.

^{13}C NMR (100 MHz, CD_2Cl_2, −100 °C) (M = major isomer, m = minor isomer, ***M*** = M and m are overlapped): δ 147.6 (M-C_a or M-$C_{a'}$), 147.3 (M-$C_{a'}$ or M-C_a and M-C_e or M-$C_{e'}$), 146.1 (m-C_a or m-$C_{a'}$), 145.8 (M-$C_{a'}$ or M-C_a), 145.6 (m-C_e or m-$C_{e'}$), 143.7 (m-$C_{a'}$ or m-C_a), 143.4 (m-$C_{e'}$ or m-C_e), 140.5 (M-C_c or M-$C_{c'}$ and m-C_c or m-$C_{c'}$), 139.4 (M-$C_{c'}$ or M-C_c), 138.7 (m-$C_{c'}$ or m-C_c), 135.1 (***M***-phenyl-*p*-C), 134.0 (Ar′-C_o), 130.2 (***M***-phenyl), 130.0 (M-C_f or M-$C_{f'}$), 129.8 (M-$C_{f'}$ or M-C_f and m-C_f or m-$C_{f'}$), 129.1 (m-$C_{f'}$ or m-C_f), 128.5 (***M***-phenyl), 128.2 (***M***-phenyl), 128 (q, $^3J_{CF}$ = 33 Hz, Ar′-C_m), 127.3 (***M***$_d$ or ***M***$_{d'}$), 127.2 (***M***$_{d'}$ or ***M***$_d$), 125.6 (M-C_b or M-$C_{b'}$), {124.8, 124.7, 124.6} (***M***$_b$ or ***M***$_{b'}$), 123.8 (q, $^1J_{CF}$ = 273 Hz, Ar′-CF_3), 122.4 (***M*** phenyl-*ipso*-C), 117.0 (Ar′-C_p), 108.4 (d, J_{CH} = 155 Hz, M-Ar**C**H═CH_2), 107.5 (d, J_{CH} =

(62) Brookhart, M.; Grant, B.; Volpe, A. F. *Organometallics* **1992**, *11*, 3920.

(63) de Graaf, W.; Boersma, J.; Smeets, W. J. J.; Spek, A. L.; van Koten, G. *Organometallics* **1989**, *8*, 2907.

(64) Morse, P. M.; Spencer, M. D.; Wilson, S. R.; Girolami, G. S. *Organometallics* **1994**, *13*, 1646.

(65) Binsch, G. In *Dynamic Nuclear Magnetic Resonance Spectroscopy*; Jackman, L., Cotton, F. A., Eds.; Academic: New York, 1975; p 77.

(66) March, J. *Advanced Organic Chemistry*, 3rd ed.; John Wiley & Sons: New York, 1985.

(67) Hammett, L. P. *Physical Organic Chemistry*, 2nd ed.; McGraw-Hill: New York, 1970; p 356.

(68) Taylor, J. R. *An Introduction to Error Analysis*; University Science Books: Mill Valley, CA, 1982.

(69) Byers, P. K.; Canty, A. J. *Organometallics* **1990**, *9*, 210.

Table 6. Olefin Rotational Barriers of **2H** and **2OCH$_3$** in CD_2Cl_2 at −70 °C[a]

X	W_1 (Hz)	W_{-1} (Hz)	k_1 (s^{-1})	k_{-1} (s^{-1})	$\Delta G^{\ddagger}_1$	$\Delta G^{\ddagger}_{-1}$	$\Delta G°$
H	8.3 ± 1	15.5 ± 1	21 ± 7	44 ± 6	10.5	10.2	0.2[b]
OCH_3	9.1 ± 1	13.2 ± 1	24 ± 6	37 ± 5	10.5	10.3	0.2[b]

[a] W_o = 1.5 ± 1 Hz. [b] Calculated from the −90 °C spectrum. $\Delta G‡$ and $\Delta G°$ are in units of kcal/mol. $\Delta G‡$ ± 0.1 kcal/mol.

Table 7. Yields and CHN Analyses for (phen)Pd(η^3-CH(CH_2CH_3)C_6H_4-*p*-X)$^+$Ar′$_4$B$^-$

		analyses found (calcd)		
X	yield (mg)	%C	%H	%N
H	265, 90%	50.16 (50.16)	2.39 (2.46)	2.14 (2.21)
CH_3	241, 81%	50.30 (50.55)	2.29 (2.59)	2.11 (2.18)
OCH_3	239, 82%	49.79 (49.93)	2.45 (2.56)	2.23 (2.16)
Cl	191, 63%	49.18 (48.84)	2.29 (2.32)	1.87 (2.15)
CF_3	320, 99%	49.02 (48.51)	2.55 (2.26)	2.14 (2.10)

163 Hz, m-Ar**C**H═CH_2), 75.3 (dd, J_{CH} = 165 Hz, J_{CH} = 155 Hz, m-ArCH═**C**H_2), 73.4 (t, J_{CH} = 161 Hz, M-ArCH═**C**H_2), 18.9 (q, J_{CH} = 134 Hz, M-CH_3), 14.6 (q, J_{CH} = 136 Hz, m-CH_3). $^1J_{CH}$ could not be resolved in the phenanthroline region due to the close proximity of the resonances and the large $^2J_{CH}$ (6−7 Hz). Missing aromatic styrene resonances are obscured by overlapping Ar′ or phen resonances.

(b) NMR Analysis of Complex 1 plus 1.5 Equiv of Styrene. A 5 mm NMR tube was charged with **1** (10 mg, 8.0 × 10^{-6} mol). CD_2Cl_2 (0.7 mL) was added at −78 °C, and the sample warmed briefly to dissolve **1**. Styrene (1.5 μL) was added at −78 °C. The sample was placed in a cold (−80 °C) NMR probe and a ^{1}H NMR spectrum recorded. Only one set of resonances was observed for free and coordinated styrene (1.8 equiv total by integration) together with one set of resonances for an unsymmetrical palladium complex.

^{1}H NMR (300 MHz, CD_2Cl_2, −80 °C): δ 8.76 (d, J_{ab} = 5.3 Hz, 1H, H_a), 8.60 (d, J_{ac} = 8.22 Hz, 1H, H_c or $H_{c'}$), 8.48 (d, $J_{a'c'}$ = 8.22 Hz, 1H, $H_{c'}$ or H_c), 8.34 (d, J = 4.95 Hz, 1H, $H_{a'}$), 7.96 (d, $J_{dd'}$ = 9.0 Hz, 1H, H_d or $H_{d'}$), 7.94 (d, $J_{dd'}$ = 9.0 Hz, 1H, H_d or $H_{d'}$), 7.92 (dd, J_{ab} = 5.3 Hz, J_{bc} = 8.22 Hz, 1H, H_b), 7.80 (dd, $J_{a'b'}$ = 4.95 Hz, $J_{b'c'}$ = 8.22 Hz, 1H, H_b), 7.73 (m, 8H, Ar′-H_o), 7.50 (m, 5.8H, Ar′-H_p + styrene-Ar), 7.3 (m, 7.2H, styrene-Ar), 6.90 (dd, J = 16.6 Hz, J = 9.6 Hz, 1.8H, styrene vinyl), 5.44 (d, J = 16.6 Hz, 1.8H, styrene vinyl), 5.08 (d, J = 9.6 Hz, 1.8H, styrene vinyl), 0.85 (s, 3H, CH_3).

Determination of Olefin Rotational Barriers in 2H and 2OCH$_3$. Samples of **2H** and **2OCH$_3$** were prepared as described for the ^{1}H NMR sample of **2H**. The sets of resonances for the major and minor isomers merged as the temperature was raised. The line widths of the CH_3 resonances for these isomers were measured and the rate constants for their interchange calculated from $k_{ex} = \pi(W - W_o)$ at −70 °C; W = line width at half-height of resonance undergoing exchange, W_o = natural line width in absence of exchange (Table 6).

Reaction of 1 with *p*-X-Styrene: Synthesis of (1,10-Phenanthroline)Pd(η^3-CH(Et)C_6H_4-*p*-X)$^+$Ar′$_4$B$^-$ (X = CF_3, Cl, H, CH_3, OCH_3) (3X). In a representative synthesis, **1** was prepared *in situ* from the addition of CH_2Cl_2 (2 mL) to (phen)Pd(CH_3)$_2$ (74 mg, 2.33 × 10^{-4} mol) and $H^+(OEt_2)_2$Ar′$_4$B$^-$ (253 mg, 2.50 × 10^{-4} mol) at −30 °C. After 30−60 min all of the insoluble orange (phen)Pd(CH_3)$_2$ had been consumed, leaving a yellow solution (sometimes a slurry). *p*-X-Styrene (1 equiv) was added and the solution warmed to 20 °C and stirred for 15 min. The solvent was removed *in vacuo* and the product (oil or solid) dissolved in CH_2Cl_2 (0.5 mL) and cooled from −30 to −78 °C (hexane (0.3 mL) was added to X = Cl, CF_3 at −30 °C), yielding a crystalline material. The mother liquor was removed and the crystals were washed at −78 °C with CH_2Cl_2 (2 × 0.5−1 mL) and hexanes (2 × 1−3 mL). Yields and analyses are reported in Table 7; ^{1}H and ^{13}C NMR data are recorded in Tables 9 and 10.

Synthesis of Isotopomers of 3H: 3-*d*$_{11}$ and 3-^{13}*C*. Complexes **3**-d_{11} and **3**-^{13}C were prepared in an analogous manner to **3H**.

Dynamic Behavior of 3H. (a) Rate of Exchange of the Ortho Hydrogens Measured by Spin Saturation Transfer.[45,70] A 5 mm NMR tube was charged with **3H** (20 mg, 1.6 × 10^{-5} mol) and CD_2Cl_2 (0.7 mL) and placed in a precooled NMR probe (300 MHz, −2 °C). The T_1 constant of the ortho hydrogen at δ 6.69 (H_x) was determined using a standard inversion recovery sequence (Bruker AMX software) with 16 τ ranging from 100 ms to 16 s, T_1 = 2.92 s. The other ortho hydrogen at δ 7.30 (H_y) was saturated; the integral of H_x decreased to 64 ± 1% of its original value determined relative to $CHDCl_2$ (15 s delay between pulses). Two control experiments were conducted. First, a saturation pulse was applied upfield of H_x by $\nu_x - \nu_y$ (180 Hz) at −2 °C, with no effect, to test if the decrease in H_x was due to the power of the saturation pulse. Second, H_y was saturated at −40 °C to test for an NOE contribution to the change in the integral of H_x; no NOE was observed. The rate of exchange was calculated from the Forsén and Hoffman expression: $k_{ex} = (1/T_1) \times ((M^o - M^\infty)/M^\infty)$; M^o = area of H_x without saturation of H_y, M^∞ = area of H_x with saturation of H_y; k_{ex} = 0.6 ± 0.1 s^{-1}, $\Delta G^{\ddagger}$ = 12.2 ± 0.1 kcal/mol.

(b) H/D Scrambling in (phen)Pd(*anti*-η^3-CD(CD_2CH_3)(C_6D_5)$^+$. A 5 mm NMR tube was charged with **1** (30 mg, 2.5 × 10^{-5} mol). CH_2Cl_2 (0.7 mL) was added at −78 °C and the sample warmed briefly to dissolve **1**. Styrene-d_8 (2.8 μL, 0.93 equiv) was added and the sample placed in an ice bath. After 5−10 min, the sample was placed in a warm NMR probe (29.4 °C) and the isotopomerization observed by ^{2}H{^{1}H} NMR spectroscopy.

Reaction of 3H with Styrene (a) Formation of (1,10-Phenanthroline)Pd(CH(CH_3)C_6H_5)$^+$ (4). A 5 mm NMR tube was charged with **4** (252 mg, 1.99 × 10^{-4} mol), CD_2Cl_2 (0.7 mL), and styrene (40 μL, *ca.* 1.5 equiv). After sitting overnight, there was a small amount of black Pd present; the ^{1}H NMR spectrum showed complete conversion to product. Hexane (0.3 mL total) was added to the tube and the solution cooled to −78 °C for 2 days, after which the mother liquor was removed and the remaining solid washed at −78 °C with CH_2Cl_2 (2 × 0.5 mL) and hexane (3 × 0.7 mL) to remove styrenes. The solid was then dissolved in CH_2Cl_2 (1 mL) and cannulated onto Celite. The filter aid was washed with CH_2Cl_2 (10 mL). The solvent was removed *in vacuo*, and the product was dissolved in CH_2Cl_2 (0.5 mL) and cooled overnight at −78 °C, giving crystals of **4**. The mother liquor was removed, the crystals were washed with CH_2Cl_2 (2 × 0.5 mL) and hexane (2 × 1 mL), and the product was dried *in vacuo*. Isolated yield: 110 mg, 48%. Anal. Calcd for $C_{52}H_{29}B_1F_{24}N_2Pd_1$: C, 49.77; H, 2.33; N, 2.23. Found: C, 51.06; H, 1.86; N, 2.77. ^{1}H and ^{13}C NMR data are reported in Tables 9 and 10.

(b) Determination of the Equilibrium Constant for 3H + Styrene = 4 + (*E*)-β-Methylstyrene. A 5 mm NMR tube was charged with **4** (20 mg, 1.59 × 10^{-5} mol), CD_2Cl_2 (0.7 mL), and (*E*)-β-methylstyrene (33 μL, 2.54 × 10^{-4} mol). The tube was flame sealed and the ^{1}H NMR evaluated until equilibrium was attained (*ca.* 1 day) at 20 °C. The equilibrium constant was calculated from K_{eq} = [(*E*)-β-methylstyrene][**4**]/[styrene][**3H**]; the concentrations were determined by the ^{1}H relative integrals (80 scans with 30° flip angle using a 10 s delay between pulses). K_{eq} = 249 ± 4, and ΔG° = −3.2 kcal/mol.

(c) Reaction of Styrene-*d*$_8$ with 3H. CD_2Cl_2 (0.7 mL) was added to a 5 mm NMR tube charged with **3H** (10 mg, 8 × 10^{-6} mol). Styrene-d_8 (0.8 equiv) was added and the sample placed in a 20 °C NMR probe. The initial slow disappearance of **3H** was observed together with the appearance of a broad resonance at δ 1.47 (CHD_2), followed by an appearance of a singlet at δ 3.75 (Ar-CH).

(d) Kinetic Study of the Reaction of 3H with Styrene. A 2 mL solution of **3H** (100.9 mg, 7.96 × 10^{-5} mol) and CD_2Cl_2 (0.0265 M) was prepared. Aliquots (0.7 mL) were placed in four 5 mm NMR tubes. At −78 °C, variable amounts of styrene were added with a microliter syringe to the NMR tubes. The samples were shaken, in order to dissolve styrene frozen on the inner surface of the tube, and placed in a precooled (−2 °C) NMR probe. ^{1}H NMR spectra were

Table 8. Summary of Kinetic Data for **3H** + Styrene

[**3H**]	[styrene] (M)	volume of styrene (μL)	$10^4 k_{obsd}$ (s^{-1})	[**3H**]	[styrene] (M)	volume of styrene (μL)	$10^4 k_{obsd}$ (s^{-1})
0.0124	0.175	15	1.2	0.0248	0.548	50	2.6
0.0122	0.278	30	2.1	0.0232	0.999	100	3.9
0.0119	0.519	45	2.6	0.0218	1.495	150	4.6
0.0117	0.638	60	3.2	0.0206	1.839	200	5.4

(70) Mann, B. E. *J. Magn. Reson.* **1976**, *21*, 17.

Table 9. ^{1}H NMR Data for (phen)Pd(η^3-CH(R)C_6H_4-*p*-X)$^+$Ar′$_4$B$^-$

X (R)	$H_{a,a'}$	$H_{b,b'}$	$H_{c,c'}$	$H_{d,d'}$	$H_{\beta,\beta'}$
H^y (ET)	9.12 (dd, 5.0, 1.5 Hz)	7.97 (dd, 8.3, 5.0 Hz)	8.61 (dd, 8.3, 1.5 Hz)	8.01 (d, 8.4 Hz)	7.30 (d, 7.8 Hz)
	8.39 (dd, 4.9, 1.5 Hz)	7.81 (dd, 8.3, 4.9 Hz)	8.51 (dd, 8.27, 1.5 Hz)	7.96 (d, 8.4 Hz)	6.69 (d, 7.4 Hz)
$CH_3{}^y$ (Et)	9.12 (dd, 5.0, 1.5 Hz)	7.98 (dd, 8.3, 5.0 Hz)	8.62 (dd, 8.3, 1.5 Hz)	8.00 (d, 9.0 Hz)	7.25 (d, 8.1 Hz)
	8.35 (dd, 4.9, 1.5 Hz)	7.84 (dd, 8.3, 4.9 Hz)	8.52 (dd, 8.3, 1.5 Hz)	7.98 (d, 9.0 Hz)	6.65 (d, 7.4 Hz)
$OCH_3{}^y$ (Et)	9.12 (dd, 5.0, 1.5 Hz)	7.96 (dd, 8.3, 5.0 Hz)	8.61 (dd, 8.3, 1.5 Hz)	8.00 (d, 8.9 Hz)	6.76 (dd, 8.1, 2.2 Hz)
	8.30 (dd, 4.9, 1.5 Hz)	7.82 (dd, 8.3, 4.9 Hz)	8.51 (dd, 8.3, 1.5 Hz)	7.98 (d, 8.9 Hz)	7.36 (dd, 9.1, 2.1 Hz)
Cl^z (Et)	9.10 (dd, 5.0, 1.4 Hz)	7.99 (dd, 8.2, 5.0 Hz)	8.65 (dd, 8.2, 1.4 Hz)	8.0 (m)	7.23 (d, 7.2 Hz)
	8.43 (dd, 5.0, 1.4 Hz)	7.90 (dd, 8.2, 5.0 Hz)	8.56 (dd, 8.2, 1.4 Hz)	overlapped with $H_{b,b'}$	6.73 (d, 7.6 Hz)
$CF_3{}^y$ (Et)	9.10 (dd, 5.0, 1.5 Hz)	7.99 (dd, 8.3, 5.0 Hz)	8.64 (dd, 8.3, 1.5 Hz)	8.01 (d, 8.9 Hz)	7.24 (br, d)
	8.38 (dd, 4.9, 1.5 Hz)	7.87 (dd, 8.3, 4.9 Hz)	8.56 (dd, 8.3, 1.5 Hz)	8.00 (d, 8.9 Hz)	6.84 (br, d)
H^y (Me)	9.11 (dd, 4.9, 1.5 Hz)	7.81	8.63 (dd, 8.4, 1.5 Hz)	8.0 (m)	7.5 (under Ar′-H_o)
	8.4 (dd, 4.9, 1.5 Hz)	7.7 (under Ar′-H_p)	8.52 (dd, 8.4, 1.5 Hz)		6.43 (br, d, 6.9 Hz)

X	$H_{\gamma,\gamma'}$	ArCH	CH_2	CH_3	X
H^y	under Ar′ at 7.72)	4.06 (dd, 8.6, 6.8 Hz)	2.0 (multiplet)	1.37 (t, 7.3 Hz)	under $H_{d,d',b}$ at ca. 8.0
$CH_3{}^y$	7.58 (d, 7.6 Hz)	3.98 (dd, 8.0, 7.4 Hz)	1.9 (multiplet)	1.35 (t, 7.3 Hz)	2.37 (s)
	under Ar′ at 7.72				
$OCH_3{}^y$	7.09 (dd, 8.1, 2.6 Hz)	3.87 (dd, 9.0, 6.4 Hz)	1.9 (multiplet)	1.31 (t, 7.3 Hz)	4.00 (s)
	7.21 (dd, 8.7, 2.6 Hz)				
Cl^z	under Ar′ at 7.72	4.10 (dd, 10.4, 5.2 Hz)	1.9 (multiplet)	1.35 (t, 7.4 Hz)	
$CF_3{}^y$	under $H_{d,d',b}$ at ca. 8.0	4.31 (dd, 10.0, 5.4 Hz)	2.0 (multiplet)	1.37 (t, 7.4 Hz)	
H^z (Me)	under $H_{d,d',b}$ at ca. 8.0	3.95 (q, 6.7 Hz)		1.52 (d, 6.7 Hz)	

[a] ^{1}H NMR (^{y}300 or ^{z}400 MHz, CD_2Cl_2, 20 °C); Ar′4B$^-$: δ 7.7 (m, 8H, H_o), 7.5 (s, 4H, H_p).

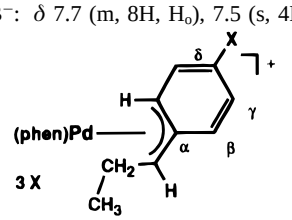

obtained over at least two half-lives. The methine signals of **3H** and **4** were monitored. Rate constants were obtained as the slope of the line of ln(**3H**-CH/(**3H**-CH + **4**-CH)) vs time. The concentrations of styrene and **3H** were corrected for the additive change in volume caused by the addition of styrene by combining the volume of styrene and solution (0.7 mL). This experiment was repeated at *ca.* one-half the concentration (0.0127 M) of **3H**. A summary of the kinetic data is given in Table 8 and the *ca*. 0.02 M data plotted in Figure 3. The limiting rate constant was obtained as the inverse of the intercept of the plot of $1/k_{obsd}$ vs 1/[styrene]. The reported k_{lim} is the average from the two sets of data below. $k_{lim} = (8.8 \pm 0.5) \times 10^{-4}$ s^{-1}, and $\Delta G^{\ddagger} = 19.6 \pm 0.1$ kcal/mol.

(c) Double Label Crossover Experiment: 3-d_{11} + 3-^{13}C. A 5 mm NMR tube was charged with **3**-d_{11} (15 mg, 1.2×10^{-5} mol) and **3**-^{13}C (15 mg, 1.2×10^{-5} mol). CD_2Cl_2 (0.7 mL) was added at −78 °C. The sample was shaken briefly to dissolve the solids and placed in a precooled NMR probe (−2 °C). No crossover was observed after 90 min at −2 °C and 1 week at 20 °C as judged by the lack of (1) decrease of the CH resonance, (2) appearance of $^{12}C^1\mathbf{H}_n{}^2H_{2-n}$ between the $^{13}C\mathbf{H}_2$ signals in the ^{1}H NMR spectrum, and (3) $^1J_{^{13}CD}$ in the $^{13}C\{^1H\}$ NMR spectrum.

Kinetics of the Migratory Insertion Reactions of (1,10-phenanthroline)Pd(CH$_3$)(η^2-CH$_2$=C(H)C$_6$H$_4$-*p*-X)$^+$Ar′$_4$B$^-$ (X = H, CH$_3$, OCH$_3$, Cl, CF$_3$) (2X). CD_2Cl_2 (0.7 mL) was added to a 5 mm NMR tube charged with **1** (10 mg, 8×10^{-6} mol) at −78 °C. The sample was warmed briefly to dissolve **1**, then styrene (0.9 μL, 0.9 equiv) was added at −78 °C. The sample was placed in a precooled NMR probe (−29.2 °C). The phenanthroline signals were broadened in the intermediate exchange regime. The integrals of the decreasing H_c and H_t signals of **2X** and the increasing CH, CH_2, and H_o resonances of **3X** were monitored relative to the unchanging $CHDCl_2$ or Et_2O resonance. The reaction was followed for two half-lives. Rate constants were obtained from slopes of plots of −ln[**2X**$_t$] or −ln[**3X**$_\infty$ − **3X**$_t$] vs time (s). The averaged rate from two separate experiments is reported. ^{1}H NMR data of **2X** at −29.2 °C are reported in Table 11.

Temperature-dependent studies of the migratory insertion of **2H** were similarly performed. Averaged rate constants, from two kinetic runs, and the temperatures at which they were obtained are reported in Table 3.

Synthesis of (1,10-Phenanthroline)Pd(CH$_3$)(NC-3,5-(CF$_3$)$_2$C$_6$H$_3$)$^+$-Ar′$_4$B$^-$ (9). CH_2Cl_2 (2 mL) was added to (phen)Pd$(CH_3)_2$ (148 mg, 4.67×10^{-4} mol) and H$^+$(OEt$_2$)$_2$Ar′$_4$B$^-$ (525 mg, 5.19×10^{-4} mol) at −30 °C. After 20 min 3,5-$(CF_3)_2$-benzonitrile (79 μL, 5.1×10^{-4} mol) was added. Following an additional 30 min at −30 °C, the yellow solution was warmed to 20 °C and stirred for 15 min. The solution was cooled to between −40 and −50 °C, and hexanes (0.1 mL) were added, yielding a colorless crystalline product. At −78 °C, the mother liquor was removed and the product washed with CH_2Cl_2 (2 × 0.5 mL) and hexanes (5 mL). The product was warmed to 20 °C, washed with additional hexanes (5 mL) and dried *in vacuo*, yield 598 mg (91%). Anal. Calcd for $C_{54}H_{26}BF_{30}N_3Pd$: C, 46.20; H, 1.87; N, 2.99. Found: C, 46.24; H, 1.84; N, 2.87.

^{1}H NMR (300 MHz, CD_2Cl_2, 20 °C): δ 8.94 (dd, J_{ab} = 5.3 Hz, J_{ac} = 1.4 Hz, 1H, H_a), 8.87 (dd, $J_{a'b'}$ = 4.9 Hz, $J_{a'c'}$ = 1.5 Hz, 1H, $H_{a'}$), 8.68 (dd, J_{bc} = 8.3 Hz, J_{ac} = 1.4 Hz, 1H, H_c), 8.63 (dd, $J_{b'c'}$ = 8.3 Hz, $J_{a'c'}$ = 1.5 Hz, 1H, $H_{c'}$), 8.44 (br s, 2H, NCAr′-H_o), 8.40 (br s, 1H, NCAr′-H_p), 8.09 (d, $J_{dd'}$ = 9.0 Hz, 1H, H_d), 8.07 (d, $J_{dd'}$ = 9.0 Hz, 1H, $H_{d'}$), 7.97 (dd, J_{bc} = 8.3 Hz, J_{ab} = 5.2 Hz, 1H, $H_{b'}$), 7.95 (dd, $J_{b'c'}$ = 8.3 Hz, $J_{a'b'}$ = 4.9 Hz, 1H, $H_{b'}$), 7.71 (m, 8H, Ar′-H_o), 7.54 (s, 4H, Ar′-H_p), 1.43 (s, 3H, CH_3).

^{13}C NMR (75 MHz, CD_2Cl_2, 20 °C): δ 162.3 ($^1J_{CB}$ = 50 Hz, Ar′-C_i), 149.7 (d, J_{CH} = 185 Hz, C_a or $C_{a'}$), 148.9 (d, J_{CH} = 183 Hz, $C_{a'}$ or C_a), 148.4 (s, C_e or $C_{e'}$), 144.5 (s, $C_{e'}$ or C_e), 140.6 (d, J_{CH} = 168 Hz, C_c or $C_{c'}$), 139.7 (d, J_{CH} = 167 Hz, $C_{c'}$ or C_c), 135.3 (d, J_{CH} = 161 Hz, Ar′-C_o), 134.4 (q, $^2J_{CF}$ = 36 Hz, NCAr′-C_m), 133.9 (q, $^3J_{CF}$ = 3.8Hz, $^1J_{CH}$ (d) = 172 Hz, NCAr′-C_o), 131.4 (s, C_f or $C_{f'}$), 130.8 (s, $C_{f'}$ or C_f), 130.0 (d, J_{CH} = 170 Hz, NCAr′-Cp), 129.4 (q, $^2J_{CF}$ = 29 Hz, Ar′-C_m), 128.3 (d, J_{CH} = 167 Hz, C_b or $C_{b'}$), 128.0 (d, J_{CH} = 168 Hz, $C_{b'}$ or C_b), 126.3 (d, J_{CH} = 170 Hz, C_d or $C_{d'}$), 125.8 (d, J_{CH} = 171 Hz, $C_{d'}$ or C_d), 125.0 (q, $^1J_{CF}$ = 272 Hz, Ar′-CF_3), 122.4 (q, $^1J_{CF}$ = 273 Hz, NCAr′-

Table 10. ^{13}C NMR Data for (phen)Pd(η^3-CH(R)C$_6$H$_4$-*p*-X)$^+$Ar′$_4$B$^-$

X(R)	$C_{a,a'}$	$C_{e,e'}$	$C_{c,c'}$	$C_{f,f'}$	$C_{b,b'}$	$C_{d,d'}$	X(R)
H (Et)	152.0 (d, 184 Hz) 149.4 (d, 185 Hz)	146.5 145.2	139.9 (d, 168 Hz) 139.6 (d, 167 Hz)	130.8 130.5	128.1 (d, 166 Hz) 127.9 (d, 167 Hz)	126.4 (d, 169 Hz) 126.2 (d, 170 Hz)	H (Et)
CH_3 (Et)	152.1 (d, 184 Hz) 149.4 (d, 184 Hz)	146.5 145.2	139.8 (d, 167 Hz) 139.5 (d, 167 Hz)	130.8 130.5	128.0 (d, 167 Hz) 127.9 (d, 167 Hz)	126.4 (d, 170 Hz) 126.1 (d, 169 Hz)	CH_3 (Et)
OCH_3 (Et)	152.1 (d, 185 Hz) 148.4 (d, 184 Hz)	146.3 145.4	139.8 (d, 167 Hz) 139.5 (d, 167 Hz)	130.7 130.5	128.0 (d, 167 Hz) 127.9 (d, 167 Hz)	126.4 (d, 170 Hz) 126.1 (d, 169 Hz)	OCH_3 (Et)
Cl (Et)	152.1 (d, 185 Hz) 149.9 (d, 184 Hz)	146.5 145.1	140.1 (d, 168 Hz) 139.8 (d, 168 Hz)	130.8 130.6	128.1 (d, 168 Hz) 127.9 (d, 167 Hz)	126.5 (d, 171 Hz) 126.4 (d, 170 Hz)	Cl (Et)
CF_3 (Et)	152.2 (d, 185 Hz) 150.1 (d, 184 Hz)	146.6 145.2	140.4 (d, 168 Hz) 140.1 (d, 168 Hz)	131.0 130.8	128.2 (d, 167 Hz) 128.1 (d, 167 Hz)	126.5 (d, 173 Hz) 126.5 (d, 171 Hz)	CF_3 (Et)
H (Me)	151.6 (d, 184 Hz) 149.4 (d, 184 Hz)	146.6 145.1	139.9 (d, 167 Hz) 139.6 (d, 166 Hz)	130.7 130.5	128.0 (d, 167 Hz) 127.9 (d, 167 Hz)	126.5 (d, 170 Hz) 126.2 (d, 170 Hz	H (Me)

X	$C_{\beta,\beta'}$	$C_{\gamma,\gamma'}$	C_δ	CH-Ar	CH_2	CH_3	X
H (Et)	107.7 (d, 163 Hz) 105.3 (d, 162 Hz)	134.5 (d, 162 Hz) 134.0 (d, 165 Hz)	131.7 (d, 163 Hz)	65.7 (d, 149 Hz)	23.8 (d, 149 Hz)	14.6 (q, 130 Hz)	
CH_3 (Et)	108.7 (d, 162 Hz) 105.9 (d, 161 Hz)	134.5 (d, 161 Hz) 134.0 (d, 161 Hz)	143.2	64.8 (d, 149 Hz)	23.9 (t, 128 Hz)	14.6 (q, 128 Hz)	22.6 (q, 128 Hz)
OCH_3 (Et)	112.6 (d, 164 Hz) 109.1 (d, 163 Hz)	119.5 (d, 177 Hz) 115.9 (d, 163 Hz)	162.9	63.7 (d, 155 Hz)	24.0 (t, 128 Hz)	14.7 (q, 128 Hz)	56.4 (q, 145 Hz)
Cl (Et)	107.7 (d, 165 Hz) 107.6 (d, 164 Hz)	133.9 (d, 169 Hz)	137.2	65.8 (d, 152 Hz)	23.9 (t, 129 Hz)	14.6 (q, 128 Hz)	
CF_3 (Et)	106.7 (d, 164 Hz) 103.8 (d, 170 Hz)	131.7 131.4 (broad)	132.7 (q, $^2J_{CF}$ = 33 Hz)	67.8 (d, 156 Hz)	23.9 (t, 129 Hz)	14.6 (d, 127 Hz)	124.3 (q, $^1J_{CF}$ = 273 Hz
H (Me)	115.1 (d, 165 Hz) 96.2 (d, 160 Hz)	134.9 (d, 164 Hz) 134.0 (d, 165 Hz)	131.6 (d, 165 Hz)	57.4 (d, 154 Hz)		14.9 (d, 128 Hz)	

[a] ^{13}C NMR (100 MHz, CD_2Cl_2, 20 °C); Ar′$_4$B$^-$: δ 162.3 (q, $^1J_{CB}$ = 50 Hz, C_i), 135.3 (d, J_{CH} = 159 Hz), 129.4 (q, $^2J_{CF}$ = 33 Hz, C_m), 125.0 (q, $^1J_{CF}$ = 272 Hz, CF_3), 117.9 (d, J_{CH} = 164 Hz, Cp). See Table 9 for labeling scheme.

Table 11. ^{1}H NMR[a–c] Data for (phen)Pd(CH_3)(*p*-X-C$_6$H$_4$CH=CH$_2$)$^+$ (**2X**) in CD_2Cl_2 at −29 °C

X	C_6H_4	H_g	H_c	H_t	Pd-CH_3	X
H	7.65 (d, 7.9 Hz), 7.35 (m)	7.16 (dd, 15.6, 8.7 Hz)	5.21 (d, 15.6 Hz)	4.98 (broad)	0.98 (broad)	7.35 (m)
CH_3	under Ar′ at 7.54, 7.15 (d, 7.6 Hz)	under C_6H_4 at 7.15	5.16 (d, 15.8 Hz)	4.98 (broad)	0.97 (broad)	2.28 (s)
OCH_3	7.59 (d, 8.5 Hz), 6.86 (d, 8.8 Hz)	7.16 (dd, 15.3, 7.8 Hz)	5.08 (d, 15.8 Hz)	4.87 (broad)	0.95 (broad)	3.75 (s)
Cl	7.58 (d, 8.4 Hz), 7.5 (d, 8.4 Hz)	7.09 (dd, 15.7, 8.2 Hz)	5.17 (d, 15.6 Hz)	5.01 (broad)	0.92 (broad)	
CF_3	7.75 (d, 8.7 Hz), 7.62 (d, 8.7 Hz)	7.12 (dd, 15.7, 8.6 Hz)	5.25 (d, 15.8 Hz)	5.18 (broad)	0.93 (broad)	

[a] The major and minor styrene isomers are in rapid equilibrium on the NMR time scale, causing some of the resonances to appear broadened. [b] 300 MHz. [c] Ar′4B$^-$, δ 7.7 (m, 8H, H_o), 7.5 (s, 4H, H_p); phenanthroline, δ 9-7 (complex band shape due to rotation of major and minor isomers of **2X**).

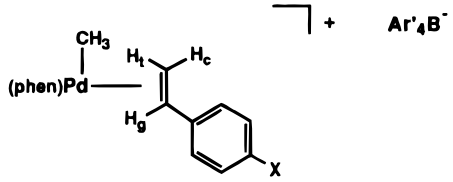

CF_3), 120.2 (s, N**C**Ar′), 117.9 (d, J_{CH} = 164 Hz, Ar′-C_p), 112.3 (s, NCAr′-C_i), 4.8 (q, J_{CH} = 136 Hz, CH_3).

Competitive Binding Studies: 9 + *p*-X-Styrene (X = CF$_3$, Cl, H, CH$_3$, OCH$_3$). In a representative experiment, a 5 mm NMR tube was charged with **9** (10 mg, 7.1×10^{-6} mol) and CD_2Cl_2 (0.7 mL). *p*-X-Styrene was added at −78 °C and the sample placed in a −66 °C probe; the ^{1}H NMR spectrum was obtained employing a 10 s delay between pulses. This was repeated for additional amounts of *p*-X-styrene (CF_3: 4, 10, 14 μL; Cl: 4, 8, 12 μL; H: 3, 6 μL; CH_3: 1.5, 3, 5 μL; OCH_3: 1.5, 3, 5). The average equilibrium constant, K_{AX} = [**2X**]-[NCAr′]/[**9**][*p*-X-styrene], was obtained seperately from the population normalized integrals of the methyl and aromatic (phen and NCAr′) resonances of these species and then averaged together. A list of average K_{AX} is reported in Table 4.

X-ray Structure Determinations. Data were collected on a Rigaku AFC 6/S diffractometer with graphite-monochromated Mo Kα radiation (λ = 0.710 73 Å) using a $\theta/2\theta$ scan; reflections with $I > 2.5\sigma$ were considered observed and included in subsequent calculations. The structures were solved by direct methods. Refinement was by full-matrix least squares with weights based on counter statistics. Hydrogen atoms were included in the final refinement using a riding model with thermal parameters derived from the atom to which they are bonded. Crystal data and experimental conditions are given in the supporting information. All computations were performed using the NRCVAX suite of programs.[71,72]

Acknowledgment. We are grateful to The National Institute of Health (2-RO1-GM28938) and the Dept. of Energy (FG05-94ER14459) for financial support of this work. F.C.R. was supported in part by a Dept. of Education Fellowship.

Supporting Information Available: Tables listing atomic coordinates, Bisos, and bond distances and angles for non-hydrogen atoms of **1** and **3H** (14 pages). This material is contained in many libraries on microfiche, immediately follows this article in the microfilm version of the journal, can be ordered from the ACS, and can be downloaded from the Internet; see any current masthead page for ordering information and Internet access instructions.

JA9527434

(71) Gabe, E. J.; Le Page, Y.; Charland, J.-P.; Lee, F.; White, P. S. *J. Appl. Crystallogr.* **1989**, *22*, 384.
(72) Johnson, C. K. Technical Report No. ORNL-5138; Oak Ridge National Laboratory: Oak Ridge, TN, 1976.